Review

Laser-Assisted Forming of Ultra-High Strength Steels: A Critical Review of Mechanisms, Processes, and Future Directions

Jimmy Gunawan-Goullet de Rugy [1], Zeran Hou [1,*], Yujie Gu [1], Lei Cen [1], Zhou Wang [2], Jianfeng Wang [2] and Junying Min [1]

[1] School of Mechanical Engineering, Tongji University, Shanghai 201804, China;
jimmy.gunawan-goullet_de_rugy@ensam.eu (J.G.-G.d.R.); 2410397@tongji.edu.cn (Y.G.); 2430403@tongji.edu.cn (L.C.);
junying.min@tongji.edu.cn (J.M.)

[2] General Motors Global Research & Development, Shanghai 201206, China; zhou.wang@gm.com (Z.W.);
jeff.wang@gm.com (J.W.)

* Corresponding author. E-mail: zeranhou@tongji.edu.cn (Z.H.)

ABSTRACT: Ultra-high strength steels (UHSS) are critical for lightweighting in the automotive and aerospace industries, but their poor room-temperature formability presents a significant manufacturing barrier. Laser-assisted forming (LAF) has emerged as a key enabling technology that utilizes localized laser heating to reduce forming forces, enhance ductility, and mitigate springback. This paper provides a critical review of the state-of-the-art in LAF of UHSS. It begins by elucidating the governing principles, including the coupled thermo-mechanical and metallurgical mechanisms such as thermal softening, dynamic microstructure evolution, and non-equilibrium phase transformations. The review then systematically surveys the major LAF process variants—including bending, roll forming, and incremental forming—and their applications in fabricating complex UHSS components. Despite its proven advantages, significant challenges impede its widespread industrial adoption. The most critical issues are identified and discussed, including local mechanical property degradation due to uncontrolled thermal cycles, the complexity of predictive multi-physics modeling, and the need for robust *in-situ* process monitoring and control. Ultimately, this review presents a forward-looking perspective, proposing future research directions that focus on microstructure management, the development of high-fidelity digital twins, and the implementation of intelligent closed-loop control systems to ensure process stability and part integrity. This work provides a comprehensive roadmap for advancing the science and technology of LAF for next-generation lightweight manufacturing.

Keywords: Laser-assisted forming; Ultra-high strength steel; Thermo mechanical coupling; Microstructure evolution; Process-structure-property relationship

1. Introduction

The rapid advancement in the automotive and aerospace industries [1] has fuelled a growing demand for materials that combine lightweight with exceptional mechanical properties to address various challenges such as reducing fuel consumption, improving payload capacity, enhancing crash-safety and extending service life [2]. Ultra-High Strength Steel (UHSS), particularly those with tensile strengths exceeding 1.5 GPA, emerged as a leading material in meeting these demands, providing a compelling combination of strength, hardness, ductility, and toughness [3]. It becomes very attractive due to its weldability and good mechanical properties [4,5]. However, the mechanical properties of these steels also pose significant challenges for traditional forming processes as they have limited formability. The lower fracture strains and the inability to sustain high levels of local deformation make it challenging to use in applications that have a cold forming method in the manufacturing process [6]. That can lead to a risk of crack formation, for example, which can pose significant problems in the industry [7]. In addition, the properties of the UHSS can result in poor room-temperature formability, characterized by severe springback. All of these obstacles can severely restrict the manufacturing of complex geometry components and hinder the full exploitation of UHSS's lightweighting potential. To overcome these obstacles, novel forming techniques, such as thermal-assisted forming techniques, have attracted

increasing attention from researchers and industry professionals. For example, hot stamping of quenched steel sheets is one such solution, offering a reduced forming load, a large amount of formability, enhanced final strength, and elimination of springback through die quenching [8]. The cold roll forming can also be a method for forming ultra-high-strength steel. Cold roll forming is a process in which thin sheets are shaped through a series of rollers with inputs at ambient temperature and without appreciable change in thickness [9].

The laser forming manufacturing process enables us to produce either uncomplicated or complicated shapes thanks to a concentrated heating source that softens the material [10,11]. It was demonstrated that a combination of laser heating and external force can increase the bending angle up to 140° and reduce the risk of rupture, springback, and edge effect [12]. It was also confirmed that the laser assisted process can reduce the process force, improve dimensional accuracy and increase formability for a range of materials [13,14]. In fact, it was shown that in the heat-affected-zone, the hardness can be considerably reduced by up to 29% and 32% [15]. Additionally, the preheating can reduce the residual stresses [16].

However, the laser cannot form the piece alone; an external force is needed [17]. To apply the necessary force to form the material, technology that uses roll forming has been studied [18]. Roll forming has the advantage of being a highly productive metal forming process [9]. In addition, Sweeney et al. have shown that the cost of a roll forming machine hour represents a small influence on the global cost of producing automotive structural parts. This means that roll forming is a low-cost process [19]. Mäntyjärvi et al. demonstrate in addition that the use of roller forming allows for forming UHSS with a 90° bend angle without damage compared to air bending [20]. A flexible and versatile incremental rolling forming process was studied by Yuan et al. by combining conventional rolling with incremental sheet forming. Compared with conventional rolling, incremental rolling has lower rolling forces, facilitating further downstream processing of sheets [21].

Considering these results, a combination of these two technologies can be the solution to the different challenges of forming a UHSS. Laser-assisted forming (LAF) has garnered significant attention due to its unique advantages of precise, localized, and rapid heating. Laser-assisted robotic roller forming of an UHSS has been developed and promising results have been obtained such as bending with no fracture [22], and a reduction in bending force and springback [23]. LAF is a localized heating technique. Earlier work by field pioneers demonstrated the basic feasibility in bending high-strength steels into shape using laser energy. Subsequent studies have expanded the applications to include a host of other processes, such as incremental forming, roll forming, and single-point forming, all of which have reported substantial improvements in formability and increased dimensional accuracy.

Laser metal additive manufacturing (AM) processes, such as selective laser melting, are also rapidly developing technologies that use laser energy to manipulate metal properties. However, they fundamentally differ in their operational principles and industrial applications.

In metal AM, the laser melts selectively powder layers to build the parts by additive manufacturing, resulting in complex geometries that cannot be achieved by conventional forming. The advantages that laser AM offers include design flexibility, rapid prototyping, and a reduction in material waste. However, due to various inherent weaknesses, such as residual stresses, anisotropy, and porosity, extensive post-processing is usually required in AM [24].

In industrial contexts, LAF applications are oriented toward the high-volume fabrication of sheet metal components with improved mechanical performance, are easily interfaced with existing forming lines, and are done with a modest capital investment. Metal 3D printing is innovative for smaller series and highly complex parts; however, it currently struggles with build size, speed, and cost for mass production [24].

Although the level of mastery of this process is increasing, the industry employs Laser-Assisted Forming (LAF) to a limited degree because severe challenges arise, such as high thermal gradients, non-equilibrium phase transformations, and uncertain effects on mechanical properties from process implementation. Heat, deformation, and microstructural changes are still not straightforward, and neither does the process control nor the mechanisms themselves tend toward the simplest forms.

Despite reviews covering various aspects of laser-assisted forming, including thermo-mechanical coupling, process variants, and specific applications in incremental forming, a literature review providing an integrated critical synthesis that considers all these angles and places LAF within the broader discourse of emerging laser-based manufacturing techniques is lacking. The main distinguishing feature of our review, compared to the previous ones focusing on single mechanisms or narrow process variants, is:

Integrative Scope: Bridging the gap between fundamental mechanisms and practical process implementations (bending, roll forming, incremental forming) with comparisons of in depth versus laser-based additive manufacturing.

Modeling Emphasis: Providing an exhaustive picture of established multi-physical modeling strategies, pointing out missing links of existing FE approaches, suggesting modeling paths for enhanced constitutive and phase-coupled simulations.

Industrial Contextualization: Contextualizing LAF with respect to recent developments in metal 3D printing (LPBF, DED) in terms of formability, cycle-time, and part quality, thus delineating unique opportunities and trade-offs for industrial uptake.

Critical Future Roadmap: Providing specific considerations on process monitoring, closed-loop control, and digital-twin development that will serve as concrete pointers for its implementation dedicated specifically to the challenges of ultra-high strength steels.

With this integrative, comparative, and forward-looking view, the review fills a critical gap in the literature, enabling researchers and engineers to utilize LAF in the next generation of laser-based manufacturing strategically.

This review aims to explore the current state of knowledge and future directions regarding the laser-assisted robotic roller forming (LRRF) of a UHSS.

2. Fundamentals of Laser-Assisted Forming

Roller forming has become a preferred technique for converting ultrahigh-strength steel sheets (exceeding 1200 MPa) into tubular profiles, such as rockers, cross-beam members, or anti-intrusion reinforcements, by continuously bending the UHSS sheet through a series of rollers to achieve the desired cross-section [22].

In the LRRF approach, a high-power laser is positioned 25 mm ahead of the roller to heat the strips to a high temperature before they undergo mechanical bending through direct contact with the roller, as shown in Figure 1a. Both the laser head and forming roller are mounted on a six-axis heavy-duty industrial robot (KR600, KUKA, Augsburg, Germany) to ensure synchronized movement, as shown in Figure 1b. The roller's path is first mapped out based on the spatial relationship between the fixture, sheet, and roller, then loaded into the KUKA smartPAD using KUKA Robot Language (KRL). These programmed motions are specified by the translation and rotation of a local Cartesian frame attached to the roller's end, relative to the global Cartesian reference. Finally, the system controller coordinates the six-degree-of-freedom joint movements to execute the process [23].
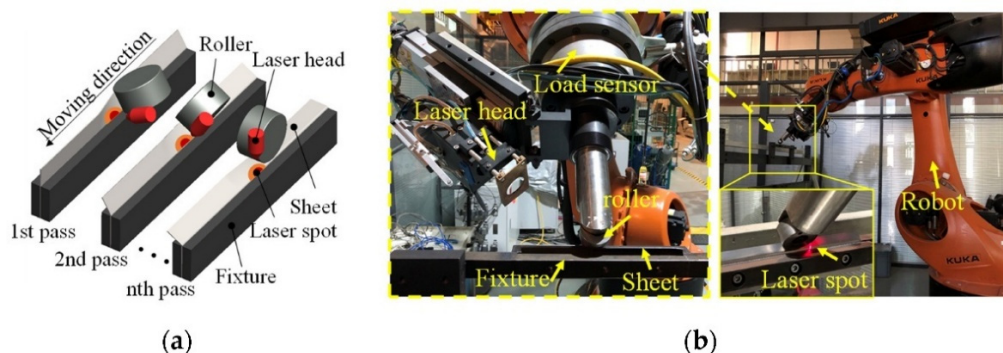

Figure 1. Laser-assisted robotic roller forming, (**a**) schematic of the forming process, (**b**) experimental setup [23].

2.1. Thermal-Mechanical-Metallurgical Coupling Mechanisms

Complex interactions between thermal input, mechanical deformation, and metallurgical phase changes characterize laser-assisted forming (LAF) processes. The localized and rapid heating from the laser generates steep thermal gradients and therefore leads to non-equilibrium phase transformations. The thermal softening mechanism usually works well when dealing with laser energy where the energy rapidly heats the deformation zone lowering the yield strength and flow stress, and hence results in less forming force. Along with this heating, one can gain ductility due to dislocation annihilation and fast recovery or re-crystallization under high-temperature deformation, which is associated with increased plastic strain before fracture. In laser-assisted robotic roller forming (LRRF) of martensitic UHSS, the outer surface of the sheet that encounters the highest temperature undergoes reverse austenitization followed by martensitic transformation upon cooling. This causes a gradient microstructure throughout its thickness such that fine-grained martensite forms at the thickest surface while tempered martensite or untempered martensite resides deeper down. Due to rapid heating, high dislocation densities and lattice defects that facilitate recrystallization and transformation kinetics remain [25].

Laser-assisted forming process needs highly coupled, multi-physics simulations that pose several challenges :

Coupling of complex physical phenomena: As Tomashchuk et al. explain for laser welding, "the interaction of high-power laser beams with metallic materials produces a number of interconnected phenomena which represent a serious challenge for numerical modeling, especially for the generation of auto-consistent models" [26]. This complexity in LAF translates into thermal, mechanical, metallurgical, and even fluid-dynamic effects being brought together in analysis.

Mesh distortion and remeshing requirements: In simulations with moving boundaries, such as those having melt pools or even the trace of a laser, mesh elements are quickly distorted. For example, Tomashchuk et al. demonstrate that mesh quality deteriorates rapidly, which is then followed by inaccurate solutions, requiring frequent remeshing to maintain fidelity [26].

Stabilization with fictitious viscosity: To suppress the unphysical flows within solid regions around the laser impact, the authors introduced fictitious viscosity into the models. However, setting this value too low or too high can either damage the accuracy of the solutions or prevent the solver from converging [26].

Mass loss problems in incompressible models: The work suggests that standard incompressible Navier–Stokes equations lead to significant mass loss during the dynamics of a keyhole. Dead loss is reduced, at the expense of being more difficult to solve, by weakly compressible formulations because of steep thermal and velocity gradients [26].

The thermal-mechanical-metallurgical coupling is modeled using a multi-element framework that links phase transformation kinetics with heat source models. This allows one to predict the temperature distribution, microstructure gradients, and deformation patterns with a high degree of accuracy field finite [25].

The development of a finite element model can be useful for optimizing and improving the processes that are able to monitor multiple parameters [27]. Thermo-metallurgical-mechanical finite element analysis (FEA) involves three fundamental components: the material's mechanical behaviour, thermal transfer, and phase change. Of these, the heat source model is of utmost significance as thermal input has a significant effect on deformation and phase changes. To efficiently model power density distribution in laser manufacturing, different models of heat sources have been developed. Double-ellipsoid volumetric heat source is the most commonly applied [28]. For the LRRF, several finite element models have been developed. Min et al. established a thermo-mechanical model using the commercial software, Abaqus 2021, to study the bending force, springback angle, and bending radius. In addition, they also investigate the effect of laser power density on the bending process and the final part profiles [23]. Liu et al. used a thermos-metallurgical-mechanical model to investigate the temperature field, microstructural evolution and plastic deformation, as shown in Figure 2 [29].
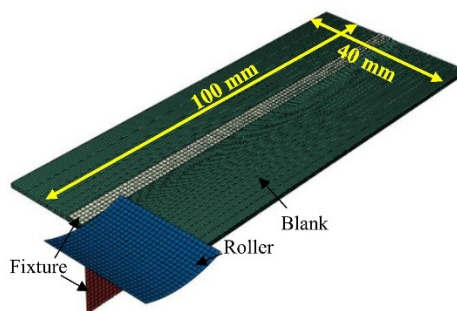

Figure 2. Assembly and mesh of LRRF [29].

To summarize, laser-assisted forming encompasses thermal, mechanical, and metallurgical effects. It works by rapidly heating the material with a laser, which softens it and subsequently reduces the forming force, thereby improving ductility through recrystallization. In the case of LRRF with martensitic UHSS, the surface undergoes reverse austenitization, resulting in fine-grained martensitic transformation and a gradient microstructure.

For LRRF modeling concerning the finite-element analysis, the basic principles include coupling heat transfer, phase transformation, and mechanical behavior. Accurate simulation using heat source models such as the double-ellipsoid has been relatively well studied, and studies have shown that laser power mainly affects deformation, temperature, and microstructure evolution.

2.2. Material Response under Localized Heating

Rapid thermal cycling induces microstructural changes such as tempering of the martensite in the heat affected zone (HAZ) of martensitic steels. Martensitic UHSS responds to localized laser heating by phase transformation and microstructural refinement. In LARF, the laser-irradiated zone is subjected to rapid heating rates, which promote the conversion of martensite to austenite. Upon subsequent cooling, refined martensite is formed due to suppressing grain growth and enhancing the nucleation rate. Dynamic recrystallization phenomena occur in the outermost layer, resulting in the development of a fine-grained high-strength structure that resists cracking and enhances bendability [25].

Xu et al. characterized heat transfer by conduction, radiation, and convection in UHSS for GTP through an experimental process. They discern three levels from heating (S1), transfer (S2), to quenching (S3). The conduction-radiation coupling causes faster temperature changes across all phases. The surface temperature increased sharply, then stabilized, while cooling exhibited a steeper drop compared to holding decreasing temperature gradients with depth [30]. These are directly useful for LRRF in that they inform the UHSS behaviour during the process.

According to Afkhami et al., in the HAZ, the hardening of unalloyed high-strength steel varies by subzone and plastic flow is best described by the Voce and Kocks-Mecking models in this context. Hardening was traced to ferritic microstructures near the fusion line and lath-like features further away [31]. These models are useful for correlating microstructure-driven hardening along laser paths and thereby providing a better understanding of the LRRF process.

The local softening allows formability under reduced stress, enhances springback response, and improves dimensional accuracy of the final component. The microstructural heterogeneity induced by LAF is directly correlated with performance enhancements in formed parts, increased energy absorption, and reduced failure risks under impact conditions [25].

In a nutshell, thermal cycling fastened and intensified the kinetics of martensite treatment of UHSS and, from the perspective of LRRF, localized laser heating will change the austenite, opaquely positioned, or disappear quickly during gem stabilization of sub-martensite matensite which is of smaller grain size and is supposed to possess reasonable strength and formability.

Laser quick heating causes significant temperature changes, whereas it is used to mark the three ways that heat moves on LRRF in terms of how the heat flow cools off. Therefore, all these improvements enhance formability, reduce forming stress, improve springback control, and increase the performance of LRRF-formed components.

2.3. Critical Process Parameters and Their Interactions

LRRF alters the stress states, such as thermal gradients, which create thermal stresses that are superimposed on mechanical stresses during formation. All process cooling leaves residual stresses, tensile in the laser-heated region and compressive in the surrounding areas, to bring the system back into balance. Therefore, it is essential to comprehend the key parameters of the LRRF.

The key parameters in LRRF include laser power, scan speed, beam diameter, incident angle, and the mechanical loading path. These govern thermal profiles, transformation kinetics, and ultimately the microstructural and mechanical properties of the formed component. For example, altering the incident angle changes the heat input distribution and subsequently the temperature field gradient. A newly developed Gaussian-uniform hybrid heat source model, specifically designed for this application, has been shown to predict these effects with a 5% deviation from experimental results [25].

Qiu et al. explored the bending of a thin-walled structure and confirmed the importance of laser power, forming passes, and scanning speed in optimizing the process for this case. It was found that laser power and scanning speed are correlated to the softening effect. Forming passes affect the magnitude of plastic deformation [32]. In addition, angle increment and moving direction can play a major role in reducing some defects such as edge waves [33]. Min et al. confirmed the prominent role of the laser power to reduce effectively the bending forces and as a result the springback angle. Some other process adjustments could be significant, such as forming at high temperature and unloading at a lower temperature [23]. Path compensation is also significant in mitigating robot stiffness deformation to prevent any inaccuracy in forming piece geometry [34].

The heating rate plays a very critical rule on the mechanism of austenite transformation. A high heating rate shifts the transformation from a diffusional process to a massive diffusionless transformation. Such a drastic change in the transformation kinetics and morphology of the resultant phases necessitates rigorous control and modelling for predictable process results [25].
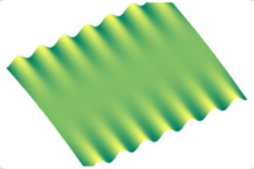
Figure 3 presents a summary of the critical process parameters.

Laser power	Controls how much thermal energy is given and therefore depth of heating, phase transformations, and softening behavior directly
Scanning speed	Governs how long heat input is exposed, determining peak temperatures, thermal gradients, and rates of cooling
Beam diameter	Influence the area of heat distribution which affects the uniformity and intensiveness of thermal treatment
Incident angle	Change the effective laser energy density on the material surface so that the shape and reach of the heated zone modify
Mechanical loading path	Determine the course of deformation and contributes to different strain distribution and the final part geometry
Forming passes	Insure the geometry accuracy of the piece and can prevent some defects
Angle increment	Influence the degree of bending per pass, thus promoting strain accumulation and likelihood of cracking
Heating rate	Controls the approaches of phase transformation and microstructural evolution affecting the mechanical properties and formability

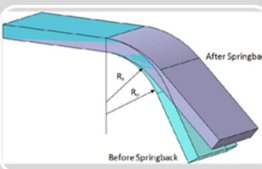**Figure 3.** Critical process parameters.

3. Challenges and Recent Solutions for Laser-Assisted Forming

The laser-assisted roller forming process was developed to address several issues that are challenging to solve with the classic bending process. Additionally, over the years, the process has undergone continuous evolution. This part will present the challenges and latest developments on the process summarized in Figure 4.
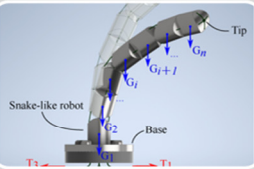

Edge waves
- Application of synchronized laser heating and 6 forming passes with a angular increment of 15°
- Decrease in forming forces that eliminate edge waves

Springback
- Application of laser heating. Application of path compensation
- Increase the bendability and the forming forces needed so lower springback

Stiffness
- 3D digital image correlation to measure the stiffness and double sided-robotic roller forming process with path compensation
- More accurate prediction of the stiffness and adjusted path compensation

Complex shapes
- Study made on hat-shaped beams, four thin-walled
- The LRRF can effectively handled the bending of complex shapes with correct springback, stiffness values and geometry accuracy

Figure 4. Summary of the challenges and latest developments on the process. Image sources from Refs. [32,35–37].

3.1. Edge Waves

The edge waves, which result from edge buckling at the strip edge, is a common defect observed in the cold roller forming process [38]. During each pass, the strip's edges follow longer spatial trajectories than its centre, causing them to stretch more. Upon leaving the stand, these edge regions undergo longitudinal compression as the strip's cross section strives to retain its original shape. This circumferential squeeze then drives expansion in both the length and thickness directions, all while preserving overall volume. As a result, during cold forming, the edges experience greater tensile strain than the rest of the strip. With continued deformation, the edge strain gradually shifts from tension to compression. Because the edges lack stability, they are prone to developing defects [39,40]. Particularly on the LRRF process, the elements ahead of the roller stretch into a three-dimensional curve. Once the roller passes, these elements are subjected to compressive stresses, which serve to maintain a straight edge. As the longitudinal plastic strain increases, the compressive stresses also increase. When these stresses exceed a critical threshold, marking the onset of compressive instability, edge buckling takes place [33].

The occurrence of edge waves is a common issue in roll forming [41]. To solve this issue, Liang et al. studied a method to control the edge wave defects during roll forming of a UHSS. It was found that the thickness of the sheet, the height of the flange, and the forming speed all influenced the edge wave defects [42].

To address this issue in the case of the LRRF, Liu et al. proposed a set of optimized forming parameters. This parameter can effectively address the issue of the edge waves. By applying synchronized laser heating, under the same forming conditions results in a 20% decrease in forming forces which can also help to eliminate the edge waves. When six forming passes are applied with a constant angular increment of 15°, laser heating eliminates edge waves. Interestingly, the LRRF with 6 forming passes creates a remarkably similar specimen's edge profile to the one made with reciprocating motion and the downhill technique [33].

In summary, edge waves are primarily generated at the strip edges due to buckling along the edges of the strip, which is a common type of defect in cold roll forming. This defect occurs due to non-uniform strain distributions, which involve greater stretch at the edges compared with the center and a subsequent collapse. However, this behavior is modified by laser heating in the LRRF process. Where the roller precedes in the line of action of the forming pass, elements are stretched. Behind the roller, these elements are compressed, thereby intensifying the compressive stress with forming passes. When the critical value determined within the material is exceeded, edge buckling occurs.

LRRF, usually synchronized laser heating, reduced the forming force by up to 20% and also managed to eliminate edge waves. This significant advancement in quality of edges is facilitated by using six passes with 15° increments, which is comparable to results derived from more complicated methods, such as reciprocating motion.

3.2. Springback

Another common defect is the springback shown in Figure 5. This phenomenon is due to the elastic recovery of the piece during the unloading [43]. It was found that springback tends to increase in roll forming with the material strength [44]. In addition, residual stress is also a major factor that affects springback [45]. The roller forming can effectively reduce the springback. However, the phenomenon persists when forming the piece [46], particularly when trying to form a UHSS [47].
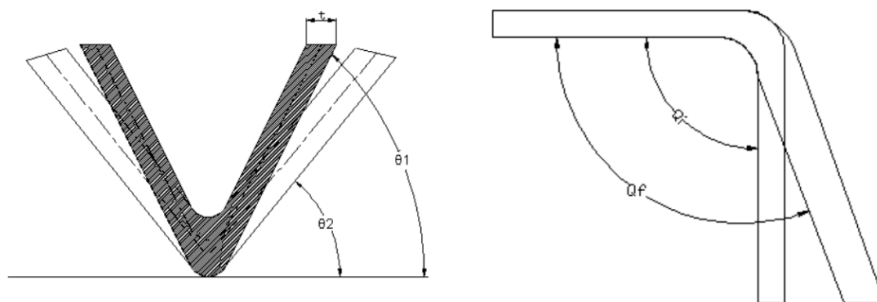

Figure 5. Principle of springback [48].

Springback depends on many factors such as the properties of the material and the processing conditions. To obtain the desired size and shape, the prediction of the springback is a crucial factor [49]. Badr et al. applied a new constitutive model, the HAH-model, to analyse the springback behaviour during the roll forming. The model was able to predict the

springback behaviour of the material with high accuracy [50]. Chongthairungruang et al. indicate that the Yoshida-Uemori kinematic hardening model, when applied in simulations, can provide an accurate prediction of the springback effect [51]. Neural network solutions can also serve as a tool to predict, control, and manage the springback [52].

It has been proven that the laser can improve the formability of metals. Gisario et al. discovered that the superimposition of thermal and mechanical mechanisms can significantly reduce the extent of the springback at the end of the bending process. The springback has been reduced about 10 times on titanium and 30 times on aluminium [53]. It was demonstrated by Grèze et al. that, in fact, the effect of temperature is beneficial in reducing the stress gradient, which is the primary factor in springback formation [54].

Applied to the LRRF, it was proved that the laser heating markedly lowers springback by reducing the required forming forces, and implementing path compensation enables the successful shaping of tight, thin-walled profiles with acute bend radii which are decreased without laser heating by 33.3% and 35.0%. Min et al. showed that LRRF can reduce bending forces by 43%, which is achieved through a compact profile with high precision. Figure 6 shows that the most significant improvement in springback can be obtained with a laser power density between 5 and 7.5 J/mm^2. In that study, LRRF can produce a piece with a springback angle of less than 1°, thanks to an optimized laser power density of 10 J/mm^2. Additionally, forming at higher temperatures and unloading at lower temperatures can also play a role in reducing springback [23]. Qiu et al. revealed that the influence of process parameters on springback and bend radii parallels their impact on forming forces. In contrast, the number of passes has a negligible effect on springback. Springback, which results from the release of elastic deformation, shows a positive correlation with forming forces. Consequently, it can be markedly reduced by increasing the laser power and lowering the scanning speed, as we can see in Figure 7a,b.

In contrast, increasing the number of forming passes has a minimal effect on springback, as shown in Figure 7a,b. With the process fine-tuned to a 750 W laser output, six forming passes, and a scan rate of 5 mm/s, the maximum force in LRRF decreased to approximately 2.1 kN. This adjustment also produced a more precise thin-walled profile, reducing the springback angle to approximately 4.1° and achieving a compact cross-section with a radius-to-thickness ratio of nearly 1.0 [32].

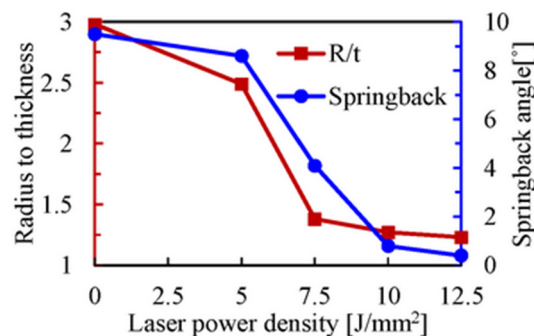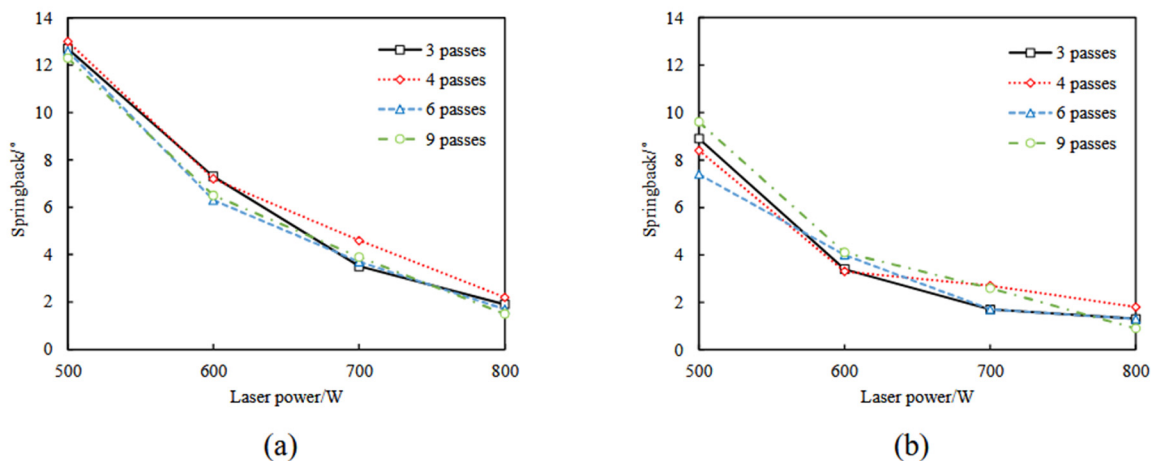**Figure 6.** Effect of laser power density on the springback angle and bending radius [23].

Figure 7. Springback under varying parameters: Springback angles of final parts by LRRF with scanning speed of (**a**) 10 mm/s and (**b**) 5 mm/s [32].

To summarize, data relating to higher forming force and spring-back indicates that laser parameters significantly influence the forming force in LRRF. Adverse effects, including a reduction in forming force and springback, are observed at higher laser power and lower scanning speeds; however, increasing the number of passes has a minimal influence on springback. Optimization at a laser power of 750 W, with 6 passes and a scan rate of 5 mm/s, minimizes the forming force to ~2.1 kN and reduces the springback angle to ~4.1°, thereby producing a thin-walled profile with greater accuracy at a radius-to-thickness ratio of ~1.0.

3.3. Stiffness

Stiffness is also a big issue when a process involves the use of industrial serial robots [55]. It is challenging to get valuable information about the stiffness of industrial robots from the manufacturer [56]. This problem can be caused by joint deformation, the transmission mechanism, friction, the environment, and many other factors. If the stiffness issue is not resolved, it can lead to irregular deviations of the robot, which in turn can result in motion errors at the manipulator ends. This impacts the machining accuracy and surface quality of the workpiece [57,58].

In the case of the LRRF, forming a UHSS is challenging because of the stiffness deformation of the industrial robot. To solve this issue, Liu et al. explored the development of a double sided-robotic roller forming process. It was found that thanks to laser heating and path compensation of robot stiffness deformation we can form compact profiles with sharp radius. The bending radii were decreased by 33.3% and 35.0% using only the path compensation values [34].

Lin et al. proposed an innovative approach to measure the stiffness of serial industrial robots with 3D digital image correlation (3D-DIC) and high precision. It used 3D-DIC to measure the complete six-degree displacement with external loads applied to the robot end-effector. The 3D-DIC takes images before and after deformation, which are called the reference image and the deformed image, respectively, in deformation analysis. The reference subset is a small portion of the reference image, and the target subset is the corresponding portion of the deformed image. Grayscale distribution techniques are used to find the target subset. A point's 3D displacement can be directly ascertained by comparing its 3D coordinates in the reference and deformed images. Joint stiffness values are identified through measurements of robot posture, displacement, and applied force data gathered. The method was experimentally verified on a KUKA KR600-2830 robot with an average relative error of 5.8%, which is significantly lower compared to traditional methods [59].

Overall, stiffness issues with industrial serial robots can significantly affect accuracy and surface finish, especially during processes such as LRRF when forming UHSS. Joint deformation, along with other factors, causes motion errors due to limited manufacturer data. Some studies have employed double-sided LRRF and robot path compensation to address this issue, which helps achieve up to a 35% reduction in bending radius.

For a better qualification of robot stiffness, an accurate method was proposed that uses 3D-DIC to measure six-degree displacement under external load. The technique generated a relative error of only 5.8% on a KUKA robot, demonstrating its superiority compared to traditional approaches.

3.4. Complex Shapes

Among the first studies made about the LRRF, a simple shape was often study, a simple bend of nearly 90° [22,23]. However, UHSS can also find application in the automobile for forming complex car parts [60]. Nevertheless, as indicated, the UHSS is particularly hard to create due to its inherent mechanical properties. That can be challenging if we want to use UHSS in complicated shapes, such as the body structural parts of a car [61].

Liu et al. study the application of the LRRF for forming dual-phase steels to hat-shaped beams by sequential flanging. Experimental findings indicate that the LRRF process can enhance the peak force, average force, and apparent stiffness of thin-walled structures by 14.5%, 12.7%, and 140%, respectively. For the four thin-walled structures, the peak force, mean force, and apparent stiffness are improved by 3.2%, 3.6%, 19.0% according to the results of C1 and C2. According to the results from cases C1 and C3, smaller bending radii lead to increases in peak force, mean force, and apparent stiffness of thin-walled structures by 9.6%, 6.3%, and 85.7%. They observed that a small bending radius has a larger impact on bending performance, particularly the pronounced stiffness of thin-walled structures fabricated using LRRF, compared to the laser-induced HAZ. The outcomes of this study present a productive way for fabricating thin-walled profiles with large bend radii from high-strength steels, along with enhanced bending properties through the LRRF process [62].

Liu et al. further investigated the three-point bending properties and geometrical shapes of thin-walled hat-section beams produced by LRRF and robotic roller formingThe results show that LRRF significantly reduces the geometric distortion caused by longitudinal tension buildup in multi-pass forming. Furthermore, the bending performance of the

LRRF beam assembly is improved in the initial stage of three-point bending. They achieved a springback angle of 0.5° and a radius-to-thickness value of 1.1. The improvement is a result of a reduced bending radius and mechanical property alteration in the laser heat-affected zone. Beams produced without the assistance of a laser are less geometrically accurate and lead to premature spot weld failure under bending tests. The beams produced by LRRF exhibit higher displacement before failure, with the cracks initiating at the boundaries of the laser-affected zone [63]. In addition, as previously mentioned, optimized parameters can help form more complex shapes. The thin-walled structure, as shown in Figure 8a, was manufactured using optimized parameters. The applied laser power was 750W, and they were able to successfully form the piece shown in Figure 8b. It was shown that the optimized process parameters reduced the peak force to around 2.1 kN. In addition, the springback angle was reduced from 11.7° to 4.1° and R/t ratio 1.0 was achieved [32].
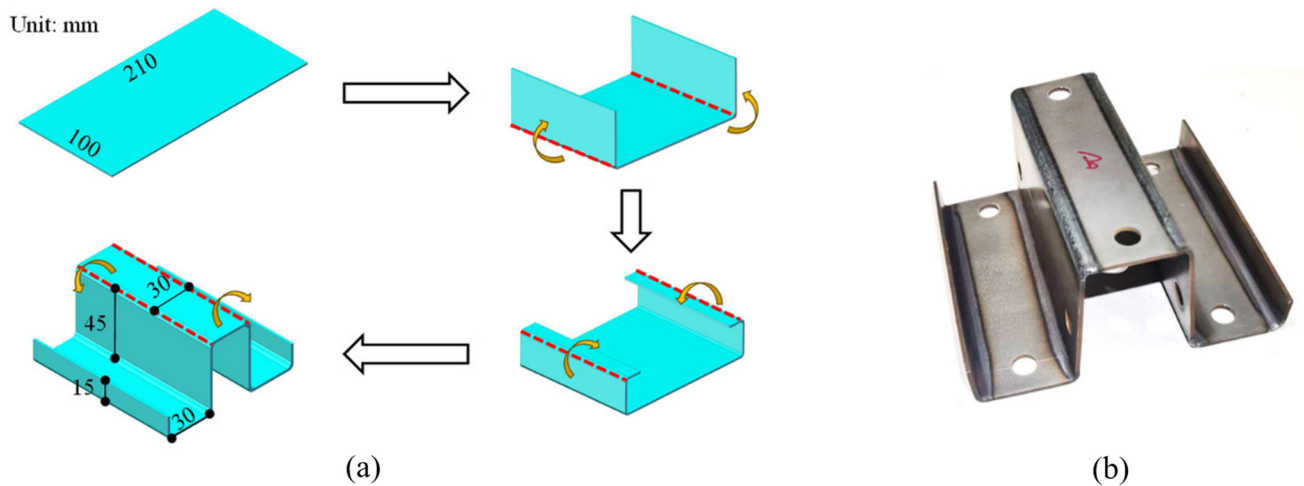

Figure 8. (**a**) Presentation of the fabrication procedure for a thin-walled structure designed for seat trails and (**b**) image of a thin-walled structure fabricated via LRRF process [32].

All in all, the LRRF mechanism enhances the performance of forming thin-walled structures with high strength steels. It showed improvements in peak force, mean force, and apparent stiffness by as much as 14.5, 12.7, and 140%, respectively, with emphasis on minor bending radii.

Three-point bending tests demonstrate that LRRF reduces geometric distortion in addition to improving accuracy in forming. A springback angle of 0.5° with an R/t ratio of 1.1 was achieved, which is known to be better compared to the so-called conventional roller forming by robots. Also, extremely complex hat-beams were successfully formed using optimized parameters.

4. Future Perspectives and Research Directions

Due to its substantial benefits in various applications, the integration of a laser energy field into the ultrahigh-strength steel (UHSS) roller forming process has garnered growing attention. LRRF is currently able to address several issues such as edge waves, springback, stiffness, and the bending of complex shapes. However, the process still needs to be improved, such as the FEM model, to predict the material's behaviour more accurately during the process or to extend the scope of its application. The key prospectives and trends are summarized in Figure 9.
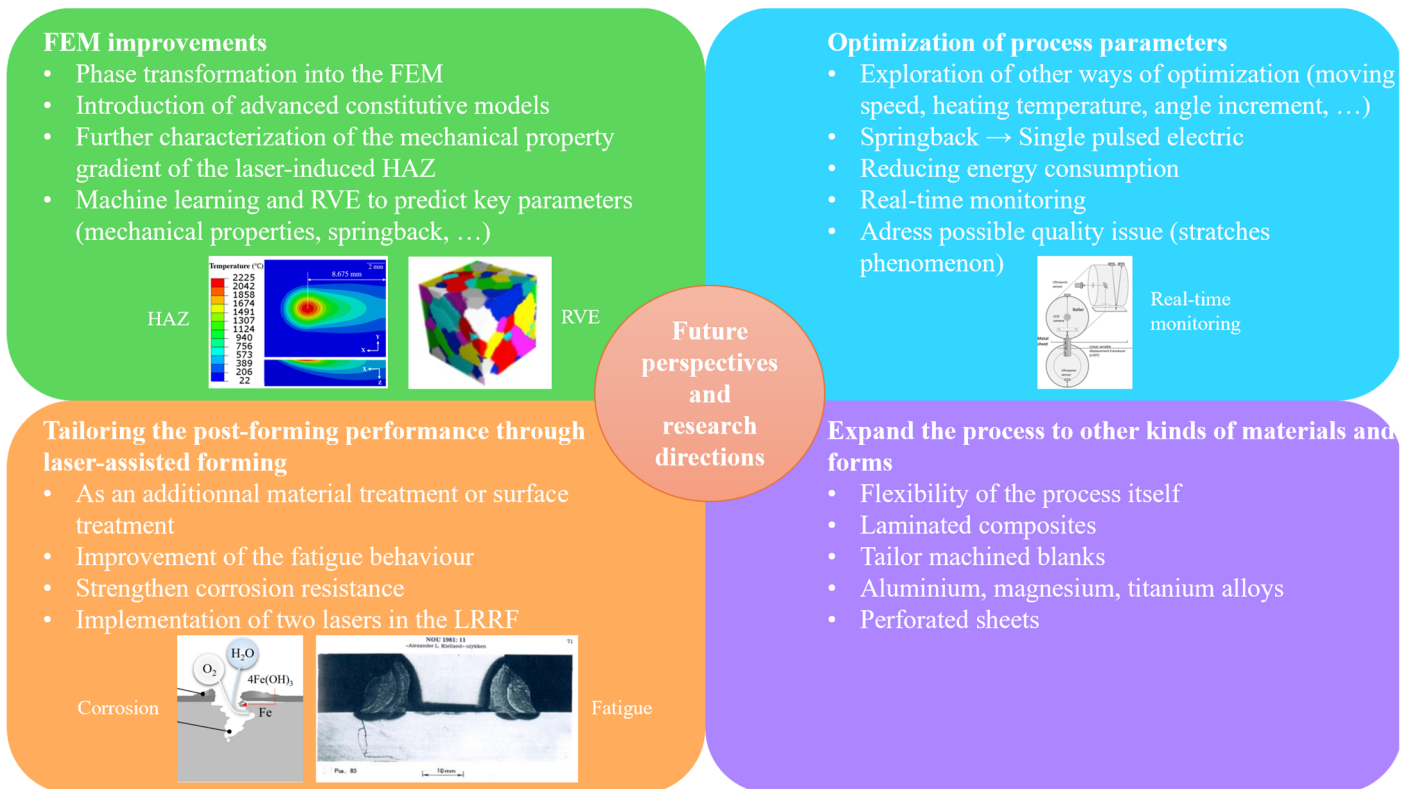
Figure 9. Future prospective and trends of LRRF. Image sources from Refs. [64–68].

4.1. Phase Transformation into the Finite Element

It was found that the microstructure has a considerable influence on the mechanical properties [69]. Liu et al. have been developing a thermo-mechanical model to simulate the LRRF process. However, the model does not account for the microstructural phase transformation [22]. It was demonstrated by Li et al. that forming ability was improved, especially after phase transformation [70]. The role of phase transformation and the mechanical properties evolutions was also emphasized by Mandal et al. As explained, the hardness, yield strength, and tensile strength improve as the cooling rate and carbon content increase [71]. It was therefore suggested that integrating phase transformation into the FE model could be the next step in the research [22]. The finite element method is an efficient solution for phase transformation computation [72].

Such implementation has already been done for other kinds of processes. He et al. used the COMSOL Multiphysics heat transfer module to introduce the temperature behaviour depending on the phase transformation, which can be absorbed to complete the phase transformation [73]. Quan et al. have implemented the phase transformation to simulate the hot stamping process of a UHSS. The material's transformation properties, more especially, the circumstances and processes by which one phase changes into another, are used to characterize the interactions between these phases. Phase transformation kinetic models provide a mathematical representation of these relationships. The previously established transformation kinetics were utilized in this situation. The Johnson-Mehl-Avrami-type kinetic equations that the software automatically generated, along with the constructed TTT diagrams, were applied to diffusion-controlled transformations, such as the transformation of austenite into ferrite, pearlite, and bainite. On the other hand, Magee's equation was used to describe the kinetics of non-diffusional transformations. Experimental results have demonstrated that the model can predict comparable outcomes [72].

Tang et al. also introduced it to the hot stamping process. They implemented the phase transformation using the Johnson-Mehl-Avrami equation to evaluate the volume fraction with some modification to consider the effect of boron. They are also known as the Koistien and Marburger equation to describe the non-diffusion type transformation as a function of temperature. The hardness distribution is calculated using empirically based equations as a function of steel composition and cooling rate. The hardness of the different phases was then calculated through the hardness computation model [74]. Ghafouri et al., on the other hand, used it to simulate the welding distortion of a UHSS. The model was developed through a sequentially coupled thermos-metallurgical-mechanical formulation in the Abaqus FE code. It is highlighted that thanks to the kinetics of phase transformation, the prediction of microstructure and boundaries

of HAZ in regions whose temperatures exceeded were implemented in the analysis, which can bring additional valuable data [75].

To summarize, microstructural effects during LRRF have a considerable influence on mechanical properties. Some studies have developed a thermo-mechanical model for LRRF, but did not include consideration of phase transformations. Such transformations are otherwise important since they increase the formability and strength.

For hot stamping and welding processes, other researchers have integrated phase transformation models, such as the Johnson-Mehl-Avrami and Koistinen-Marburger equations, with FE simulations. This implementation has enabled the accurate predictions of microstructure evolution, hardness, and boundaries of the heat-affected zone. Using similar coupling approaches in LRRF would greatly enhance prediction accuracy and process optimization.

4.2. LRRF Analysis with Advanced Constitutive Models

It was mentioned that to extend the mechanical analysis of the LRRF, we should implement an advanced constitutive model to describe complicated deformation behaviour [76]. In the study, an isotropic hardening constitutive model has been referred to for mechanical simulation. Using a non-associated flow rule, the constitutive model for LRRF of UHSS combines an isotropic stress-invariant term to represent flow softening with a temperature-dependent, anisotropic fourth-order yield function. Under LRRF-relevant temperatures and strain rates, it is analytically calibrated using data on tension, compression, plane-strain, and shear. Anisotropic deformation is precisely captured by the asymmetric fourth-order plastic potential, which enables the prediction of bending profiles, springback, and residual stresses [29].

Such material behaviour, including longitudinal deformation, is implemented with an elastic-plastic finite element model with the nonlinear finite element method. That model enables the prediction of the contact arc shape and forward slip within the deformation zone and is used to analyse the impact of rolling parameters on contact profile and stress [77]. Additionally, there is a study on deformation inhomogeneity, made possible by the combination of high-fidelity crystal plasticity models with microscopic experiments. With this model, Li et al. were able to show that the deformation strain of the UHSS is non-uniform [7]. There is also the multiaxial deformation simulate through a material model which considers the influences of strain rates and adiabatic effectenable further improvement of the material failure prediction during the process. To avoid the time-consuming nature of the model, a strain-rate dependent Taylor-Quinnet-Coefficient was implemented [78].

Priest et al. introduced a modified Jonhson-Cook model to capture the non-linear thermal softening behaviour below the austenite transformation temperature [79]. This model can be adapted to capture the steep drop in yield stress observed in the laser-heated region of UHSS. Bressan et al. employed a yield stress criterion. Prediction of the forming limit strain curve was improved by using the Bressan-Barlat shear stress fracture criterion, and when calibrating the non-associated Barlat's plastic potential with seven r-values [80]. That can be used to simulate anisotropy by the LRRF if added to thermic dependency. Dao-Hang et al. proposed a constitutive model under multiaxial thermos-mechanical cyclic loading. If implemented in a simulation, it can achieve a better fit with the measured data under isothermal and non-isothermal axial-torsional cyclic loadings [81]. In the LRRF, this describes the transition of rigidity in the heated area, which is deformed by the roller. Castillo et al. proposed a rate-dependent viscoplastic model that includes a stress-dependent viscosity law. The bending angles predicted by the model agree with the experimental measurements [82]. This enables the illustration of behaviour at high temperatures and slow scanning speeds, which are the case in LRRF.

In a nutshell, for better improvement in LRRF simulations, an advanced constitutive model is necessary to describe the complex deformability of UHSS adequately. Hence, it merges isotropic hardening and a temperature-dependent anisotropic yield function with a non-associated flow rule in its constitutive model, making it very efficient to simulate flow softening, anisotropy, and springback during forming. Many modeling strategies were used to predict the behavior of UHSS such as elastic-plastic model, crystal plasticity model, Multi-axial models, modified Johnson-Cook model, Bressan-Barlat model, thermo-mechanical cyclic model, and Castillo model.

These constitutive models serve as a concrete platform for polished attributes in LRRF simulations, enabling better predictions with respect to anisotropy, residual stresses, and material failure.

4.3. Optimization of Process Parameters

Other optimization methods could be explored to correct the defects observed in the bending piece and improve process efficiency [23]. In the case of the edge waves, we could study other parameters to further eliminate the defect during the process. Parameters such as moving speed, heating temperature, and angle increment can be optimized [33].

To address the springback issue encountered during the LRRF process, an alternative approach can be explored. Song et al find that a single pulsed electric can decrease the springback angle of a UHSS sharply. The process is shown in Figure 10. Without the pulse, the springback was measured at 24.94° instead of 15.69° with the pulse. That could be explained as a consequence of stress relaxation due to the stress drop at the pulse of the electric current [83].
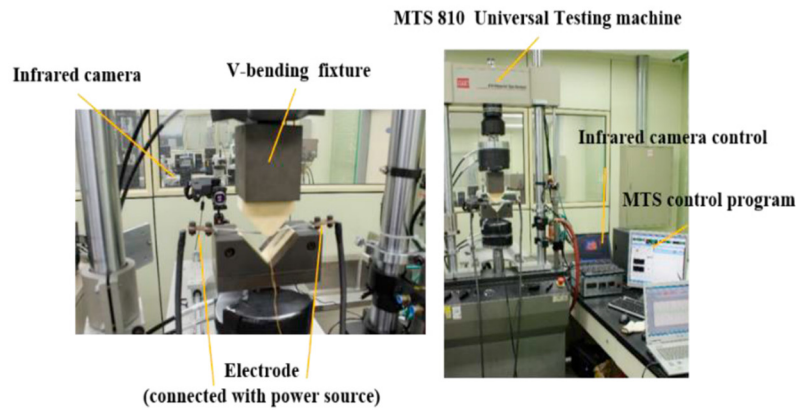

Figure 10. Image of the electrically assisted V-bending process [83].

Shirani Bidabadi et al. explore the energy consumption of the roll forming process, which is a technology used for the LRRF. It was found that the bend angle at each stand and the number of forming stands have a significant influence on reducing energy consumption by 25% [84]. In addition, Bammer addressed the optimization of temperature distribution with the goals of conserving energy, preventing undesired alterations in material properties, and reducing thermally induced deformation. His strategy is to be close to the fracture or on the maximum allowed temperature or without any heating. He showed that for a fixed energy amount, the proposed optimization can double the forming rate compared to the classic heating process [85].

Some also study the implementation of in-process monitoring in metal forming processes to make real-time adjustments to the parameters. Farshidianfar et al. developed an automated real-time thermal monitoring system to correlate microstructure, hardness, and hardening depth. The experiment used an infrared thermal camera to provide real-time thermal images, which are post-treated by the operating system. It was found that this method can be applicable in monitoring and controlling the microstructure and geometry [86].

It was suggested that for the roller, forces sensor-based, thermal sensor-based measurements or ultrasonic techniques as shown in Figure 11, could be implemented in the roller forming process to monitor for example, geometric dimension accuracy and then correct the corresponding parameters. That sensors can enable the adjustment of several process parameters in function of the force, the material temperature, and factors like friction [64].
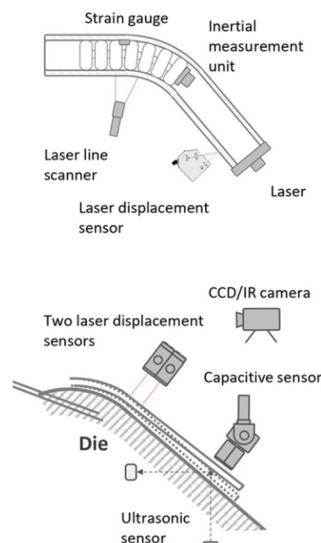

Figure 11. Application of dimension measurement with sensors within bending tools [64].

Zhang et al. suggested, in addition, the integration of machine learning to enhance the prediction and optimization of machining processes. In addition, this might help to improve the defect detection [87]. On the other hand, the use of roll forming for UHSS could also result in the scratches phenomenon that can lead to surface quality issues. A proper study about the surface quality is suggested to effectively reduce the friction condition by optimizing the parameters and improving the surface quality if the problem is identified in the LRRF [88].

To summarize, several other optimization strategies can be considered. Parameters such as moving speed, heating temperature, and angle increment can be optimized to minimize edge wave defects. Electro-assisted bending has shown potential in overcoming springback by significantly reducing springback angles through stress relaxation induced by pulsed electric current. Roll forming can save energy up to 25% by optimizing bend angles and the number of forming stands. The aim of temperature distribution optimization is to save energy, prevent degradation of material, and lower thermal deformation, thereby doubling the forming rate. In-process monitoring enables real-time adjustments to control microstructure, hardness, geometry, and forces, thereby enhancing the accuracy and stability of the process when thermal cameras and sensors are employed. Machine learning can effectively enhance prediction, optimization, and defect detection. Several additional studies should also be directed toward examining surface quality issues such as scratches during LRRF, optimizing friction conditions, and minimizing surface defects.

4.4. Characterization of the Mechanical Property Gradients of the Laser-Induced Heat-Affected-Zones (HAZ) and the Process-Structure-Performance Relationships in LRRF

Liu et al. studied the influence of bending radius and HAZ on the bending performance of an UHSS during the LRRF process. While both the reduced bending radius and the localized HAZ improve bending behaviour, finite-element simulations show that changes in the bending radius have a far greater impact, particularly on apparent stiffness, than the mechanical softening within the HAZ, according to a thorough characterization of the mechanical property gradients within the laser-induced heat-affected zone (HAZ) during laser-assisted roller forming (LRRF) of UHSS. By linking the process parameters and the ensuing HAZ-induced property gradients to the structural response and bending performance during LRRF, the study further links these observations. They conclude that future work can focus on the characterization of the mechanical property gradients of the laser-induced Heat-Affected-Zones and the process-structure-performance relationships in LRRF [62].

A study has been conducted on the laser-welded joints. It presents a crystal plasticity model that provides an inversion method for crystal plasticity parameters. This model was used to characterize the mechanical properties of the processed material that depend on the different heating zones [89].

Cao et al. investigated the evolution of microstructure and mechanical properties through simulation using a thermomechanical simulator and EBSD images. They were able to highlight the differences in terms of microstructure and mechanical properties in the HAZ different regions [90]. Another paper describes the characterization and mechanical properties of QP980-DP980 laser welded joints. For example, in Figure 12a,b they are the study of the microhardness through the material as a function of the various heating areas is presented. Different conclusion have been made regarding the mechanical properties of the HAZ, and the framework could be used in our case study [91].
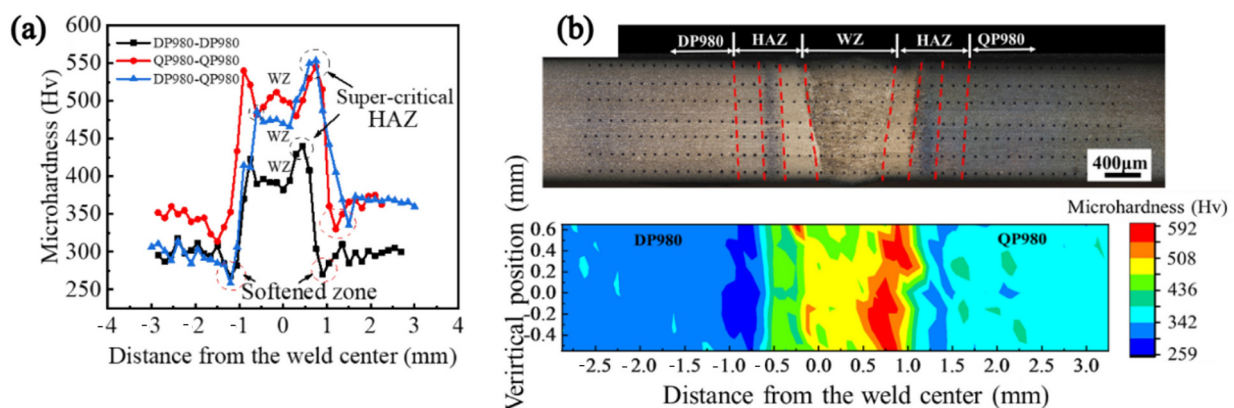

Figure 12. Microhardness (**a**) distribution and (**b**) hardness map [91].

Dong et al. investigated the mechanical properties and microstructure variation in steel after deformation subjected to hot-forming processes [92]. Singh et al. focused on the characterization and prediction of the HAZ produced by a

process that used thermal softening. They analysed the changes in the microstructure and microhardness. They used a 3D transient FEM to predict the temperature distribution for a moving Gaussian laser heat source. The model prediction has an error range of about 5–15% [93].

In summary, in the LRRF of UHSS, the effects of bending are enhanced in the presence of a localized HAZ softening and smaller bending radii. Still, the bending radius plays a more significant role in terms of stiffness. The study emphasizes the need to link process parameters, HAZ property gradients, and structural response, recommending further development of these relationships. Crystal plasticity and thermomechanical simulations elucidate variations in microstructure and hardness across the HAZ; advanced FEM and thermal models will enable the accurate prediction of such, benefitting future modeling of LRRF.

4.5. Tailoring the Post-Forming Performance through Laser-Assisted Forming

The laser can be medium to further tailor the post-forming performance by using its benefit alongside the LFFR process. In fact, the laser, as a local heating can, if the process parameters have been carefully selected, be used as a heat treatment [94]. In fact, parameters like heating rate can play a major role in the evolution of the microstructure and then in the mechanical properties [95].

In the Liu et al. study, it was shown that a comprehensive understanding of tailoring the post-forming performance through laser-assisted forming is crucial [63]. Another way to exploit the laser apart from using it to soften the material is to use it as an additional material treatment. Various technologies exist, such as laser texturing processes and laser cladding. This can have advantages in terms of hardness, intermolecular bonding, and wear resistance through the microstructural changes [96]. A paper indicates that we can also improve the fatigue behaviour by selectively melting an alloy. It was demonstrated that heat treatment through the laser can considerably improve the fatigue performance of the material, which demonstrates a good performance of the heat-treated material [97]. The effects of laser polishing were studied and Lee et al. demonstrated improved fatigue resistance in the case of a post-processing method for additive manufactured components [98].

Laser surface remelting offers a promising approach to enhance the mechanical properties and corrosion resistance. It was demonstrated that there is a reduction in corrosion density, accompanied by an increase in charge transfer resistance, compared to an untreated material [99]. Liang et al. explored the use of a laser cladded coating. Laser cladding is an effective method for surface strengthening. It was showed that they can achieved an excellent forming quality with no defects such as pores and cracks [100]. The laser can also be used as a laser surface transformation hardening post-processing in the sector of automotive [101]. Rahmand Rashid et al. used the laser as a laser reheat treatment in order to repair some damaged UHSS. It was found that this treatment can effectively control the microstructure by tuning the reheat parameters [102].

To improve the mechanical properties, the development of the LFFR with two lasers can also be explored. Wang et al. developed a two lasers process to achieve a homogeneous microstructure while avoiding overheating. A ferritic stainless steel has been studied, and the developed process allows an improvement in microhardness that is 90% higher, a 60% increase in yield stress, and 45.8% in ultimate tensile stress [103]. We can imagine a further study with a UHSS and deployment to the LFFR.

To sum up, laser technologies in LRRF are not designed solely to soften. They can be arranged in a way to improve post-forming performance due to the heat treatment, which occurs through controlled localized heating. Literature has shown that the heating rate plays a key role in determining microstructure and its properties, which affect fatigue, wear, hardness, and corrosion resistance, thereby increasing mechanical strength. Different methods like laser cladding, surface remelting, and polishing can repair and also control the microstructure. The dual-laser methods have been able to enhance mechanical properties, especially in stainless steel, which can have potential applications in UHSS LRRF.

4.6. LRRF Process for Other Kinds of Materials and Forms

The current study pramirly focuses on the use of the LRRF for bending a UHSS [22,23]. However, as an emerging manufacturing process, many other papers appear to increase the scope of the laser forming process [12] and, by extension, the LRRF.

Stewens et al. established an analytical model for the tool centre point placement in robotic roller forming. In fact, it was observed that in the case of forming other materials then UHSS, a defect appears that shapes the profile like that of a hook. To make the process more flexible, they studied a repeatable and reproducible analytical model. The key benefit is that they can reduce the hook defect which results a reduce average peak force by 25.6% and the deviation by

56.1% [104]. Laminated composites have gained great interest in the industry. Hossein Seyedkashi et al. studied the laser bending of a laminated composite. The thin copper mid-layer studied can enhance the electrical conductivity of the composite, making it adaptable to the microelectronics and aerospace industries. Nevertheless, the mid-layer decreased the rate of bending pass due to the high thermal conductivity of copper alloy. This issue can be overcome using the laser due to the copper mid-layer, which enables higher power without melting. It was found that a decrease in laser velocity results in an increase in bending angle. At the same time, a 25% increase in power improved the bending performance by about 94% [105].

Safari. et al. studied the laser bending of tailor machined blanks. They concluded that the use of a laser can help with the bendability of the piece. In fact, with an increasing laser power, the bending angle increased due to the induced heat flux, which enables the plastic deformation areas to increase [106]. Kotobi et al. examined the laser forming of St–Ti bilayer sheets. They observed that the bending angle increases when the laser power and the number of scanning passes are raised, or when the scanning velocity is lowered. The process can also increase the surface microhardness at the heat-affected zone [107]. The laser bending of perforated sheets, as shown in Figure 13, was investigated. The results indicate that using larger punch diameters reduces the bending angle in laser-formed perforated sheets. Increasing the laser scanning speed also lowers the bending angle, as does a smaller laser beam diameter [108]. Others suggested the use of the laser for bending an aluminium alloy [109], a magnesium alloy [110], and a titanium alloy [111].
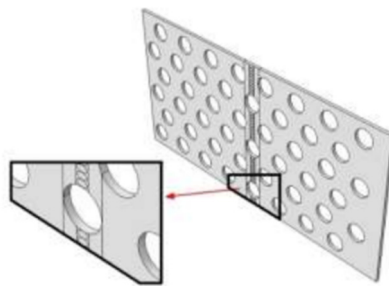

Figure 13. Schematic of the perforated sheet [108].

In summary, laser-assisted forming is applicable to numerous materials. An analytical model for robotic roller forming was developed from the research that reduced hook defects and lowered peak force and force variation. For laminated composites, increasing electrical conductivity has decreased bending efficiency. This can be improved with enhanced laser power. Increasing the laser power and decreasing the scanning speed resulted in improved bending angles and surface hardness for tailor-made blanks and bi-layer sheets. Laser forming was successfully demonstrated on perforated sheets, as well as on aluminum, magnesium, and titanium alloys, underscoring the importance of laser parameters such as speed, power, beam size, and material structure. Thus, LRRF can be applied to a different range of materials and geometries upon further optimization.

4.7. Improvement of the Finite Element Model

Some research used a finite element model to simulate the LRRF process. However, the construction of the model used experimental data that does not entirely recreate the real process condition. For example, a heating tensile test does not recreate the heating through the laser. That can lead to some inaccuracy in predicting certain behaviors.

To fix this issue, a path is to use the machine learning to estimate the high temperature mechanical behaviour of the UHSS. Yazici and al. have used a dataset of tensile test, and they process it through several machine learning model. The methodology is described in Figure 14a. They showed that one of the models, the gradient boosting, was able to predict accurately the mechanical value, achieving an adjusted coefficient of determination greater than 0.98 as shown in Figure 14b [112]. After that, they just need to implement the model predicted by the machine learning in the Abaqus finite element software, thanks to the VUHARD subroutine [113].
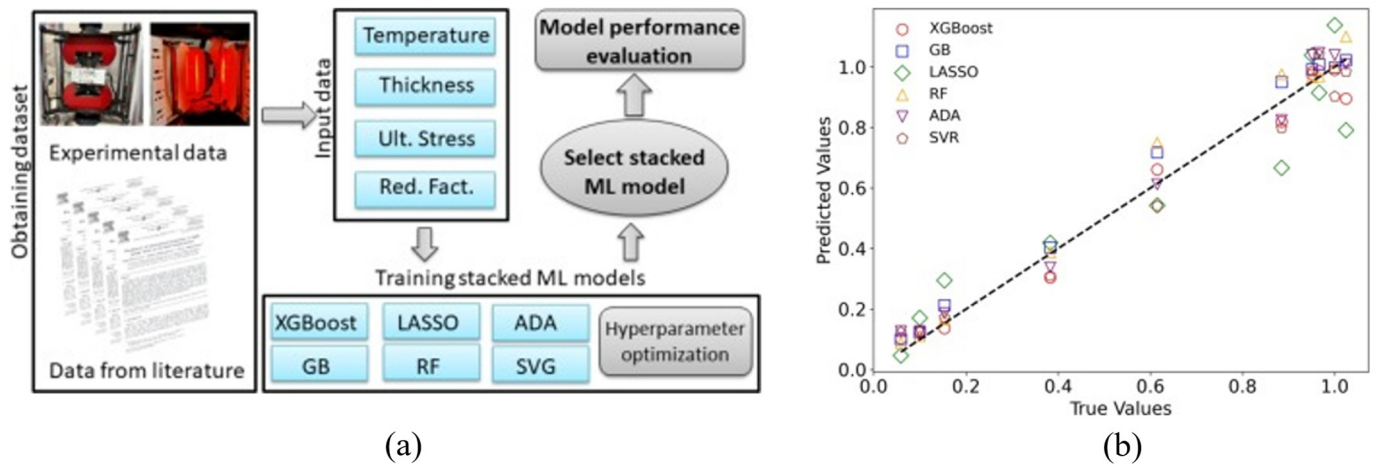
(a)

(b)

Figure 14. (**a**) Methodology used to determine the optimal machine learning model and evaluate its performance, and (**b**) scatterplot of training and testing machine learning models [112].

Another way to improve can be exploited, such as the use of a finite element analysis to predict springback [114]. This precisely consists of the springback prediction thanks to the crystal plasticity finite element model (CPFEM). The CPFEM models require less experimental characterization effort, and it has been proven that the model demonstrates significant accuracy in springback and mechanical test values [115,116]. This framework can be used on a representative volume element (RVE). To create an RVE, several electro-backscatter diffraction images are required, which provide information such as crystallographic orientation and lattice parameters [68,117], as well as the spatial distribution of grain size and phase volume fraction [118]. To maximize the amount of grain data, they specifically selected the centre of the sample surface [119]. They used Dream 3D to create the RVE based on the EBSD scans. The CPFEM was then used to predict the tensile stress-strain response of the material [120]. Then, they simply need to proceed by simulating the process to obtain the springback value [115] or the stress-strain value that can be used as a dataset for machine learning training [121]. The machine learning method can also be used to improve the springback prediction [122].

The use of artificial intelligence can also be a valuable aid in predicting some important values. Belitzki et al. studied the implantation of an Artificial Neural Network (ANN) to predict key parameters, specifically local distortions. The model was trained with a sample size of 15% which led to a prediction inaccuracy of less than 5%. In addition, the use of a genetic algorithm can be valuable for optimizing process parameters, when coupled with an Artificial Neural Network. As found, the genetic algorithm was able to identify the optimized parameters for the studied process and it was demonstrated that it is a powerful tool as it can process more than one billion potential parameter combinations [123]. In response to this result, the machine learning result could be improved by adding the ANN prediction to the predicted values dataset of the machine learning. In fact, for the case of the Random Forest Regressor for example, the final predicted value is the average of the results obtained from each branch. We can envision the implementation of ANN value prediction in conjunction with the average calculation, utilizing a coefficient that takes into account the proven accuracy of both machine learning and ANN. That could as a result improve the predicted values. Then, the genetic algorithm can be further explored in order to optimize the parameters of the LRRF to reduce defects.

To summarize, the current model suffers from some deviations from reality. To improve accuracy, we could use machine learning, which has shown good accuracy in predicting mechanical behaviour. Such predictions were subsequently integrated back into the Abaqus simulations by a VUHARD subroutine.

Another method includes springback prediction with CPFEM. CPFEM can be developed thanks to RVE formed from EBSD scans, which show crystallography, grain size, and phase distribution details. Tension-strain responses or springbacks are simulated by these same RVEs, which then serve as training data upon which ML can operate.

AI has also made some predictions shows best prospects. It was shown that local distortions were accurately predicted with ANNs, with an error of less than 5%, by using only 15% of the data. Coupling ANNs with genetic algorithms will allow an optimization of an unimaginable number of possible combinations. A hybrid approach could also be considered, where ANN predictions are combined with ML mode predictions, such as Random Forest, to achieve the highest accuracy. This is achieved by optimizing LRRF parameters with a genetic algorithm to reduce defects.

5. Conclusions

Laser-assisted forming, especially Laser-Assisted Robotic Roller Forming, is rapidly becoming a revolutionary technology for forging ultra-high strength steels into complex lightweight structures required for automotive and aerospace applications. Laser heating induces local thermal softening in the materials, allowing LAF to overcome some of the inherent disadvantages of cold forming, including high forming forces, limited ductility, substantial springback, and the chances of cracking. This critical review presents the current state-of-the-art by dissecting the intricate thermo-mechanical-metallurgical coupling mechanisms governing LAF, surveying key process variants (bending, roll-forming, and incremental forming), and evaluating solutions developed to tackle everlasting challenges such as edge waves, springback, limitations in robot stiffness, and mock-up of complex geometries.

The essence of LAF is to allow localized and very precise reduction of yield strength and flow stress that eventually results in a force reduction of almost 43%, increased formability, reduction of springback (angles of less than 1° in optimal conditions), and successful production of thin-wall profiles with small bend radii (R/t ratios approaching 1). Improvement dynamics, especially related to reverse austenitization followed by refinement to fine-grained martensite, exist within the HAZ of martensitic UHSS. These have been aided in recent years by process control improvements in synchronous laser heating, along with optimized forming paths (e.g., 6 passes at increments of 15°), along with iterative robot path compensation to reduce defects and improve geometric accuracy.

From this review, despite some advancements, it lists critical limitations regarding the research presently existing, as well as areas where knowledge is low:

Modeling Fidelity and Scope: The thermo-mechanical Finite Element Models (FEM) in existence often fail to incorporate all relevant metallurgical phase transformations and their kinetics. The absence of models such as the Johnson-Mehl-Avrami (diffusional) and Koistinen-Marburger (non-diffusional) restricts the predictability of microstructure gradients, hardness distribution, and, ultimately, the final mechanical properties and performance (e.g., fatigue, impact) of the LAF-formed parts. Present modeling often tends to be based on highly simplified constitutive behaviour (*i.e.*, isotropic hardening), which may miss important features of the complex anisotropic, rate-and-temperature-dependent flow softening and hardening behaviour of UHSS under the rapid localized cooling and heating cycles induced during LAF.

Material Scope and Property Gradients: Concentrating mainly on specific martensitic UHSS grades (e.g., QP1180), research into LAF/LRRF could extend its applicability and optimization onto a wider variety of UHSS (complex-phase, TRIP-assisted bainitic ferrite, medium-Mn steels) and other high-strength materials (Al, Mg, Ti alloys, composites). The complete characterization and predictive modeling of the mechanical property gradients across the HAZ, along with their exact correlation with process parameters and final component performance (process-structure-property relationships), requires a lot more effort. The long-term adverse consequences of these gradients, for instance, concerning fatigue and corrosion in service conditions, are poorly understood.

Process Monitoring and Control: Robust real-time *in-situ* monitoring and closed-loop control systems for LAF/LRRF are still very much in their infant stage. While there has been a proposal for utilizing thermal cameras and force ultrasonic techniques, practical integration into online measurement systems for some critical variables would include temperature distribution (on both surface and a little beneath the surface), the onset of microstructure evolution, geometric accuracy during forming, and HAZ property gradients, and make for the biggest challenge. The absence of these systems creates a rupture in process stability, repeatability, and defect prevention in already complex industrial settings.

Barriers to Industrial Implementation: Various practical barriers restrict the general acceptance. Quantification and compensation of the stiffness deformation of industrial robots under the heavy forming loads of UHSS are complicated tasks that will require advanced measurements (3D-DIC) and compensating algorithms. The sharp thermal gradients create tool life challenges and possible surface quality problems (e.g., scratches) that shall require dedicated study. The energy consumption of the laser-robot combination, although likely to become a subject for further assessment regarding sustainability due to its parameter optimization, remains a hindrance.

Long-Time Performance and Post-Processing: The review reviews the potential for the laser applied during LAF not only for softening but also for tailoring post-forming performance through controlled localized heat treatment (for instance, specific enhancement of hardness, wear resistance, and fatigue life of certain zones). However, systematic research establishing protocols for targeting specific microstructures and properties that can be achieved through optimization of laser parameters (such as power, speed, spot size, and pre/post-heating) during the LAF sequence is still not available. Mainly unexplored areas remain on LAF-induced microstructure gradients' comparison-long-term performance with conventionally formed parts, focusing on fatigue and corrosion.

Review Scope: This review, although comprehensive within its defined scope of mechanisms, processes, challenges, and future directions for UHSS LAF/LRRF, it cannot cover more aspects in exhaustive detail than others. Some specific topics, such as a detailed comparison involving all LAF variants for every UHSS grade or an exhaustive cost investigation comparing LAF with all other competing thermal forming technologies across multiple industrial contexts, lie outside the main focus of this review but should be developed further.

To elevate the limitations identified and opportunities, the specific and high-impact future research paths presented below are suggested to move forward LAF/LRRF by science and technology:

Advanced Multi-Physics Digital Twins:

- High-fidelity integrated thermo-mechanical-metallurgical simulation frameworks will be developed that incorporate the phase transformation kinetics models validated with high accuracy and advanced constitutive models such as non-associated flow rules, anisotropic yield functions (for example, Bressan-Barlat), mechanistic viscoplastic models for rate effects (for instance, Castillo's models), and crystal plasticity that connects to microstructure.
- Integrate ML with those for:
    - High-temperature flow behavior prediction with low amounts of experimental data (Gradient Boosting, VUHARD subroutines in Abaqus).
    - Springback prediction accuracy (Crystal Plasticity FEM-ML).
    - Process parameter optimization (laser power, scan speed, path, pre-/post-heating) for desired response (minimal force, zero springback, desired microstructure) using AI optimization (e.g., Genetic Algorithms with Neural Networks).
- Real "digital twins" capable of virtually simulating and optimizing the full LAF/LRRF process chain before any physical trials.

Intelligent in-process monitoring and closed-loop control:

- Research and develop robust, multi-sensor systems for real-time process monitoring:
    - Temperature: Surface and subsurface estimation using high-resolution pyrometry or thermography.
    - Microstructure: Indirect methods via thermal signature analysis with ML, or proceed toward new optical techniques.
    - Geometry: Integrating vision systems or embedded sensors with tooling for online checks of dimensional accuracy.
    - Force/Torque: Accurate measurement of forming forces and robot joint torques.
- AI control algorithms (e.g., model predictive control, adaptive control) shall thereby utilize this real-time sensor data to dynamically adjust laser parameters, robot path, and forming speed during the process, thereby maintaining stability against defects (edge waves, buckling) and ensuring part quality and microstructure consistency.

Fundamental understanding of process-structure-property-performance relationships:

- Conduct systematic experimental and computational studies to quantitatively map the gradients in microstructure (phase fractions, grain size, dislocation density), hardness, residual stress, and key mechanical properties (yield strength, ductility, toughness) across the HAZ and deformation zones for different UHSS grades and LAF parameters.
- Create predictive models quantitatively linking specific LAF process parameters with these microstructural gradients and local mechanical properties.
- Investigate possible correlation between the LAF-induced microstructural gradients and performance of formed components in service conditions (especially fatigue life, energy absorption-crashworthiness, and corrosion resistance), coming up with strategies for utilizing them for performance improvement (e.g.,: harder zones at areas of high wear, softer for energy absorption).

Expanding material and application scope:

- Extend LAF/LRRF research beyond conventional martensitic UHSS to next-generation advanced high-strength steels (AHSS), medium-Mn steels, and lightweight alloys (high-strength Al, Mg, Ti alloys).
- Investigate LAF for forming complex composite materials and multi-material structures (e.g., steel-polymer composites, bi-metal sheets).
- Pursue further work on more complex 3D geometry beyond hat-sections to include doubly curved surfaces and topologically optimized structures, an endeavour that requires advanced path planning and control.
- Explore the coalescence of LAF and other processes such as additive manufacturing (hybrid manufacturing) or tailor post-LAF laser treatments (cladding, remelting, polishing) on the same platform.

Laser as a Microstructure Tailoring Tool:

- Working to move beyond softening. Active investigation and optimization of laser parameters (power density, heating/cooling rates, overlap) within LAF for attainment of specified microstructures in targeted zones on the component (e.g., controlled fractions of retained austenite for enhanced ductility and nano-precipitates for strength).
- Investigate potential opportunities for the adoption of dual-laser configurations within LAF for independent control of the laser pre-heating zone and forming zone softening, as well as post-forming heat treatment/quenching in the same pass, precisely controlling microstructure engineering and properties gradient.
- Quantify the benefits of such tailored microstructures on the performance (fatigue, wear, corrosion) of final components.

   Sustainability, Industrial Robustness, and Standardization:

- Carry out exhaustive Life Cycle Assessment (LCA) comparing LAF/LRRF routes against conventional hot forming and cold forming + post-process regimes concerning energy consumption, material utilization, and emissions.
- Prepare pathways for energy minimization through optimized temperature distribution (as in Bammer's concept) and high efficiency in laser deployment.
- Tackling the industrial side of things: Improving the models regarding robot stiffness compensation for variable loads; studying wear mechanisms and solutions on the tooling in a laser-heated environment; creating strategies to deal with surface defects (scratches); overall, increasing reliability and robustness of the system for mass production.
- Work towards developing standardized testing and characterization protocols for LAF-processed UHSS components to promote industry uptake and qualification.

LAF, particularly that of LRRF, stands on the threshold of monumental change: the dream of mass manufacturing complex high-performance components from 'difficult' materials such as UHSS is indeed to be believed. However, the metamorphosis from promising laboratory results to a reliable industrial practice entails crossing serious scientific and technological hurdles. It is in this light that some of the limitations pointed out should be addressed, mainly by introducing advanced multi-physics digital twins, intelligent closed-loop control systems, and furthering the fundamental understanding of the complicated process-structure-property-performance relationships. These limitations should be addressed through a broader approach, where advanced modeling, AI, robust sensing, and targeted experimentation work together to address existing challenges and optimize new microstructure engineering and performance. By pursuing these ambitions with concrete research directions, LAF may truly do itself justice in ascertaining a new class of lightweight, safe, and sustainable manufacturing technologies for critical industries, such as automotive or aerospace. Such movement must shift beyond the mere formation of UHSS to the intelligent manufacturing of components with properties and performance that have been precisely engineered.

Author Contributions

J.G.-G.d.R.: Methodology, Validation, Original Draft Preparation; Z.H.: Conceptualization, Writing-Review & Editing, Funding Acquisition, Project Administration; Y.G. and L.C.: Methodology, Formal Analysis; Z.W. and J.W.: Validation, Project Administration; J.M.: Writing-Review & Editing, Supervision.

Ethics Statement

Not applicable.

Informed Consent Statement

Not applicable.

Data Availability Statement

The data that support the findings of this study are available from the corresponding author upon reasonable request.

Funding

Declaration of Competing Interest

The authors declare that they have no known competing financial interests or personal relationships that could have appeared to influence the work reported in this paper.

References

1. Li J, Zhan D, Jiang Z, Zhang H, Yang Y, Zhang Y. Progress on improving strength-toughness of ultra-high strength martensitic steels for aerospace applications: A review. *J. Mater. Res. Technol.* **2023**, *23*, 172–190. doi:10.1016/j.jmrt.2022.12.177.
2. Wang X, Li W, Yao Y, Fan L, Wang J, Wang W, et al. *In-situ* alloyed ultrahigh strength steels via additive manufacturing. *Addit. Manuf.* **2023**, *77*, 103825. doi:10.1016/j.addma.2023.103825.
3. Li J, Tian J, Zhan D, Wang W, Jiang Z. Designing a new ultra-high strength steel with multicomponent precipitates under material genetic design. *J. Mater. Res. Technol.* **2024**, *33*, 4449–4461. doi:10.1016/j.jmrt.2024.10.140.
4. Arola A-M, Kaijalainen A, Kesti V, Troive L, Larkiola J, Porter D. The effect of mechanical behavior on bendability of ultrahigh-strength steel. *Mater. Today Commun.* **2021**, *26*, 101943. doi:10.1016/j.mtcomm.2020.101943.
5. Li K, Yang T, Gong N, Wu J, Wu X, Zhang DZ, et al. Additive manufacturing of ultra-high strength steels: A review. *J. Alloys Compd.* **2023**, *965*, 171390. doi:10.1016/j.jallcom.2023.171390.
6. Pokka A-P, Kesti V, Kaijalainen A. Global formability and bendability of ultra-high strength steels: Effect of mechanical properties on the strain distribution and behaviour in air-bending. *Mater. Today Commun.* **2023**, *37*, 107081. doi:10.1016/j.mtcomm.2023.107081.
7. Li F, Liu C, Cao Y, Meng Y, Xu W. Deformation inhomogeneity evolution and crack formation mechanism analysis in ultra-high strength steel by crystal plasticity simulations. *Eng. Fail. Anal.* **2024**, *163*, 108502. doi:10.1016/j.engfailanal.2024.108502.
8. Mori K, Bariani PF, Behrens B-A, Brosius A, Bruschi S, Maeno T, et al. Hot stamping of ultra-high strength steel parts. *CIRP Ann.* **2017**, *66*, 755–777. doi:10.1016/j.cirp.2017.05.007.
9. Tsang KS, Ion W, Blackwell P, English M. Industrial validation of strain in cold roll forming of UHSS. *Procedia Manuf.* **2018**, *15*, 788–795. doi:10.1016/j.promfg.2018.07.322.
10. Geiger M, Merklein M, Pitz M. Laser and forming technology—an idea and the way of implementation. *J. Mater. Process. Technol.* **2004**, *151*, 3–11. doi:10.1016/j.jmatprotec.2004.04.004.
11. Vogt S, Weisheit A, Schleifenbaum JH. Local laser softening of cold forming steels. *J. Laser Appl.* **2020**, *32*, 042020. doi:10.2351/7.0000221.
12. Safari M, de Sousa RA, Joudaki J. Recent Advances in the Laser Forming Process: A Review. *Metals* **2020**, *10*, 1472. doi:10.3390/met10111472.
13. Duflou JR, Callebaut B, Verbert J, De Baerdemaeker H. Laser Assisted Incremental Forming: Formability and Accuracy Improvement. *CIRP Ann.* **2007**, *56*, 273–276. doi:10.1016/j.cirp.2007.05.063.
14. Luo C, Zhao Y, Cao Y, Zhao L, Shan J. Effect of laser heat treatment on bending property of laser welded joints of low-alloy ultra-high strength steel. *J. Laser Appl.* **2019**, *31*, 032011. doi:10.2351/1.5089875.
15. Amraei M, Afkhami S, Javaheri V, Larkiola J, Skriko T, Björk T, et al. Mechanical properties and microstructural evaluation of the heat-affected zone in ultra-high strength steels. *Thin-Walled Struct.* **2020**, *157*, 107072. doi:10.1016/j.tws.2020.107072.
16. Sun J, Dilger K. Influence of preheating on residual stresses in ultra-high strength steel welded components. *J. Mater. Res. Technol.* **2023**, *25*, 3120–3136. doi:10.1016/j.jmrt.2023.06.181.
17. Roohi AH, Gollo MH, Naeini HM. External force-assisted laser forming process for gaining high bending angles. *J. Manuf. Process.* **2012**, *14*, 269–276. doi:10.1016/j.jmapro.2012.07.004.
18. Sedlmaier A, Dietl T. 3D roll forming center for automotive applications. *Procedia Manuf.* **2018**, *15*, 767–774. doi:10.1016/j.promfg.2018.07.319.
19. Sweeney K, Grunewald U. The application of roll forming for automotive structural parts. *J. Mater. Process. Technol.* **2003**, *132*, 9–15. doi:10.1016/S0924-0136(02)00193-0.
20. Mäntyjärvi K, Merklein M, Karjalainen JA. UHS Steel Formability in Flexible Roll Forming. *Key Eng. Mater.* **2009**, *410–411*, 661–668. doi:10.4028/www.scientific.net/KEM.410-411.661.
21. Yuan H, Li YL, Zhao GL, Liu FF, Li FY. Incremental rolling forming process to fabricate surface micro-grooves. *IOP Conf. Ser. Mater. Sci. Eng.* **2022**, *1270*, 012033. doi:10.1088/1757-899X/1270/1/012033.
22. Liu Y, Min J, Zhang J, Cai W, Carlson BE, Bobel AC, et al. Laser-assisted robotic roller forming of an ultrahigh strength martensitic steel. *J. Manuf. Process.* **2022**, *82*, 192–202. doi:10.1016/j.jmapro.2022.07.066.
23. Min J, Wang J, Lian J, Liu Y, Hou Z. Laser-Assisted Robotic Roller Forming of Ultrahigh-Strength Steel QP1180 with High Precision. *Materials* **2023**, *16*, 1026. doi:10.3390/ma16031026.
24. DebRoy T, Wei HL, Zuback JS, Mukherjee T, Elmer JW, Milewski JO, et al. Additive manufacturing of metallic components— Process, structure and properties. *Prog. Mater. Sci.* **2018**, *92*, 112–224. doi:10.1016/j.pmatsci.2017.10.001.

25. Liu Y. Investigation on the Microstructure Evolution and Multi-Field Coupling Simulation of Laser assisted Roller Forming of Martensitic Steels. Doctoral Dissertation. School of Mechanical Engineering, Tongji University, Shanghai, China, 2024.

26. The Numerical Challenges in Multiphysical Modeling of Laser Welding with ALE, (n.d.). Available online: https://www.comsol.fr/paper/the-numerical-challenges-in-multiphysical-modeling-of-laser-welding-with-ale-65721 (accessed on 8 July 2025).

27. Yang J, Sun S, Brandt M, Yan W. Experimental investigation and 3D finite element prediction of the heat affected zone during laser assisted machining of Ti6Al4V alloy. *J. Mater. Process. Technol.* **2010**, *210*, 2215–2222. doi:10.1016/j.jmatprotec.2010.08.007.

28. Goldak J, Chakravarti A, Bibby M. A new finite element model for welding heat sources. *Met. Trans. B* **1984**, *15*, 299–305. doi:10.1007/BF02667333.

29. Liu Y, Wang J, Cai W, Carlson BE, Lian J, Min J. A thermo-metallurgical-mechanical model for microstructure evolution in laser-assisted robotic roller forming of ultrahigh strength martensitic steel. *J. Mater. Res. Technol.* **2023**, *25*, 451–464. doi:10.1016/j.jmrt.2023.05.228.

30. Xu J, Li Z-J, Dai H-L. Thermal behavior analysis of UHSS rectangular plates via gradient thermoforming process under coupled heat conduction and radiation. *Therm. Sci. Eng. Prog.* **2024**, *47*, 102331. doi:10.1016/j.tsep.2023.102331.

31. Afkhami S, Amraei M, Javaheri V, Ghafouri M, Björk T, Salminen A, et al. Flow and hardening behavior in the heat-affected zone of welded ultra-high strength steels. *Weld World* **2024**, *68*, 1001–1016. doi:10.1007/s40194-024-01703-x.

32. Qiu J, Xu C, Liu Y, Han F, Min J. Experimental investigation on process parameters of laser-assisted robotic roller bending of a thin-walled structure. *IOP Conf. Ser. Mater. Sci. Eng.* **2024**, *1307*, 012010. doi:10.1088/1757-899X/1307/1/012010.

33. Liu Y, Min J, Lin J. Robotic Roller Forming Process and Strategies to Eliminate Geometrical Defect of Edge Waves. In *Forming the Future*; Daehn G, Cao J, Kinsey B, Tekkaya E, Vivek A, Yoshida Y, Eds.; Springer International Publishing: Cham, Switzerland, 2021; pp. 479–491. doi:10.1007/978-3-030-75381-8_40.

34. Liu Y, Qiu J, Wang J, Lian J, Hou Z, Min J. An iterative path compensation method for double-sided robotic roller forming of compact thin-walled profiles. *Robot. Comput. -Integr. Manuf.* **2024**, *86*, 102689. doi:10.1016/j.rcim.2023.102689.

35. Li L, Xie H, Zhang T, Pan D, Li X, Chen F, et al. Influence of intermediate roll shifting on strip shape in a CVC-6 tandem cold mill based on a 3D multi-stand FE model. *Int. J. Adv. Manuf. Technol.* **2022**, *121*, 4367–4385. doi:10.1007/s00170-022-09529-x.

36. Darmawan A, Anggono AD, Hamid A. Die design optimization on sheet metal forming with considering the phenomenon of springback to improve product quality. *MATEC Web Conf.* **2018**, *154*, 01105. doi:10.1051/matecconf/201815401105.

37. Hu J, Liu T, Zeng H, Chua MX, Katupitiya J, Wu L. Static Modeling of a Class of Stiffness-Adjustable Snake-like Robots with Gravity Compensation. *Robotics* **2023**, *12*, 2. doi:10.3390/robotics12010002.

38. Hu S, Zhao J, Liu Y. Prediction and Prevention of Edge Waves in Continuous Cold Forming of Thick-Wall High-Strength Welded Pipe. *Metals* **2025**, *15*, 455. doi:10.3390/met15040455.

39. Farzin M, Tehrani MS, Shameli E. Determination of buckling limit of strain in cold roll forming by the finite element analysis. *J. Mater. Process. Technol.* **2002**, *125–126*, 626–632. doi:10.1016/S0924-0136(02)00357-6.

40. Woo YY, Han SW, Hwang TW, Park JY, Moon YH. Characterization of the longitudinal bow during flexible roll forming of steel sheets. *J. Mater. Process. Technol.* **2018**, *252*, 782–794. doi:10.1016/j.jmatprotec.2017.10.048.

41. Zeng G, Li SH, Yu ZQ, Lai XM. Optimization design of roll profiles for cold roll forming based on response surface method. *Mater. Des.* **2009**, *30*, 1930–1938. doi:10.1016/j.matdes.2008.09.018.

42. Liang C, Li S, Liang J, Li J. Method for Controlling Edge Wave Defects of Parts during Roll Forming of High-Strength Steel. *Metals* **2022**, *12*, 53. doi:10.3390/met12010053.

43. Lokhande AM, Nandedkar VM. Effects of Process Parameters And Investigation of Springback Using Finite Element Analysis. *Int. J. Recent Dev. Eng. Technol.* **2014**, *3*, 1–5.

44. Weiss M, Marnette J, Wolfram P, Larranaga J, Hodgson P. Comparison of Bending of Automotive Steels in Roll Forming and in a V-Die. *Key Eng. Mater.* **2012**, *504–506*, 797–802. doi:10.4028/www.scientific.net/KEM.504-506.797.

45. Li Y, Wu Z, Wang D, Nagaumi H, Luo G, Feng Z, et al. Effect of mechanical properties, microstructure and residual stress on the bending springback behavior of high-strength Al–Mg–Si–Cu alloy tubes. *J. Mater. Res. Technol.* **2024**, *28*, 3609–3618. doi:10.1016/j.jmrt.2023.12.230.

46. Badr OM, Rolfe B, Weiss M. Effect of the forming method on part shape quality in cold roll forming high strength Ti-6Al-4V sheet. *J. Manuf. Process.* **2018**, *32*, 513–521. doi:10.1016/j.jmapro.2018.03.022.

47. Liu X, Cao J, Chai X, Liu J, Zhao R, Kong N. Investigation of forming parameters on springback for ultra high strength steel considering Young's modulus variation in cold roll forming. *J. Manuf. Process.* **2017**, *29*, 289–297. doi:10.1016/j.jmapro.2017.08.001.

48. Sharad G, Nandedkar VM. Spring back in Sheet Metal Bending-A Review. *IOSR-JMCE.* **2023**, *53-56*.

49. Lal RK, Choubey VK, Dwivedi JP, Kumar S. Study of factors affecting Springback in Sheet Metal Forming and Deep Drawing Process. *Mater. Today Proc.* **2018**, *5*, 4353–4358. doi:10.1016/j.matpr.2017.12.002.

50. Badr OM, Rolfe B, Zhang P, Weiss M. Applying a new constitutive model to analyse the springback behaviour of titanium in bending and roll forming. *Int. J. Mech. Sci.* **2017**, *128–129*, 389–400. doi:10.1016/j.ijmecsci.2017.05.025.

51. Chongthairungruang B, Uthaisangsuk V, Suranuntchai S, Jirathearanat S. Springback prediction in sheet metal forming of high strength steels. *Mater. Des.* **2013**, *50*, 253–266. doi:10.1016/j.matdes.2013.02.060.

52. Gisario A, Barletta M, Conti C, Guarino S. Springback control in sheet metal bending by laser-assisted bending: Experimental analysis, empirical and neural network modelling. *Opt. Lasers Eng.* **2011**, *49*, 1372–1383. doi:10.1016/j.optlaseng.2011.07.010.

53. Gisario A, Barletta M, Venettacci S. Improvements in springback control by external force laser-assisted sheet bending of titanium and aluminum alloys. *Opt. Laser Technol.* **2016**, *86*, 46–53. doi:10.1016/j.optlastec.2016.06.013.

54. Grèze R, Manach PY, Laurent H, Thuillier S, Menezes LF. Influence of the temperature on residual stresses and springback effect in an aluminium alloy. *Int. J. Mech. Sci.* **2010**, *52*, 1094–1100. doi:10.1016/j.ijmecsci.2010.04.008.

55. Racz S-G, Crenganiş M, Breaz R-E, Bârsan A, Gîrjob C-E, Biriş C-M, et al. Integrating Trajectory Planning with Kinematic Analysis and Joint Torques Estimation for an Industrial Robot Used in Incremental Forming Operations. *Machines* **2022**, *10*, 531. doi:10.3390/machines10070531.

56. Dumas C, Caro S, Garnier S, Furet B. Joint stiffness identification of six-revolute industrial serial robots. *Robot. Comput. - Integr. Manuf.* **2011**, *27*, 881–888. doi:10.1016/j.rcim.2011.02.003.

57. Wu K, Li J, Zhao H, Zhong Y. Review of Industrial Robot Stiffness Identification and Modelling. *Appl. Sci.* **2022**, *12*, 8719. doi:10.3390/app12178719.

58. Huang X, Kong L, Dong G. Modeling and Compensation of Motion Errors for 6-DOF Robotic Manipulators. *Appl. Sci.* **2021**, *11*, 10100. doi:10.3390/app112110100.

59. Lin J, Li Y, Xie Y, Hu J, Min J. Joint stiffness identification of industrial serial robots using 3D digital image correlation techniques. *Proc. Inst. Mech. Eng. Part C J. Mech. Eng. Sci.* **2022**, *236*, 536–551. doi:10.1177/09544062211002878.

60. Toyohisa S, Masaki U, Yusuke F. Development of Press Forming Technologies for Ultra-High Strength Steel Sheets Utilizing Computer Aided Engineering. *JFE Tech. Rep.* **2019**, *24*, 39–45.

61. Nishimura R, Tanaka Y, Miyagi T, Ogawa M, Otsuka K, Nakazawa Y. Development of Forming Methods for Functional Improvement of Car Body Structural Parts. *Nippon. Steel Tech. Rep.* **2019**, *122*, 13–19.

62. Liu Y, Wang J, Cai W, Lian J, Carlson BE, Hou Z, et al. Influence of Bending Radius and Heat-Affected Zones on the Bending Performance of High-Strength Thin-Walled Structures Formed by Laser-Assisted Robotic Roller Forming. In *Proceedings of the 14th International Conference on the Technology of Plasticity—Current Trends in the Technology of Plasticity*; Mocellin K, Bouchard P-O, Bigot R, Balan T, Eds.; Springer Nature: Cham, Switzerland, 2024; pp. 382–391. doi:10.1007/978-3-031-42093-1_37.

63. Liu Y, Qiu J, Wang J, Bambach M, Min J. Fabrication of thin-walled hat-shaped beams from ultrahigh strength steel by laser-assisted robotic roller forming. *Smart Manuf.* **2023**, *02*, 2340001. doi:10.1142/S273754982340001X.

64. He X, Welo T, Ma J. In-process monitoring strategies and methods in metal forming: A selective review. *J. Manuf. Process.* **2025**, *138*, 100–128. doi:10.1016/j.jmapro.2025.02.011.

65. Mokhtari E, Heidarpour A, Javidan F. Mechanical performance of high strength steel under corrosion: A review study. *J. Const. Steel Res.* **2024**, *220*, 108840. doi:10.1016/j.jcsr.2024.108840.

66. Fajri A, Prabowo AR, Muhayat N, Smaradhana DF, Bahatmaka A. Fatigue Analysis of Engineering Structures: State of Development and Achievement. *Procedia Struct. Integr.* **2021**, *33*, 19–26. doi:10.1016/j.prostr.2021.10.004.

67. Divse V, Dubey A, Deepak M. A 3D FEM-based model of laser heating for selection of process parameters in laser-assisted machining of Ti6Al4V. *Res. Squa.* **2022**.doi:10.21203/rs.3.rs-2051569/v1.

68. Bargmann S, Klusemann B, Markmann J, Schnabel JE, Schneider K, Soyarslan C, et al. Generation of 3D representative volume elements for heterogeneous materials: A review. *Prog. Mater. Sci.* **2018**, *96*, 322–384. doi:10.1016/j.pmatsci.2018.02.003.

69. Ali M, Porter D, Kömi J, Eissa M, El Faramawy H, Mattar T. Effect of cooling rate and composition on microstructure and mechanical properties of ultrahigh-strength steels. *J. Iron Steel Res. Int.* **2019**, *26*, 1350–1365. doi:10.1007/s42243-019-00276-0.

70. Li FF, Fu MW, Lin JP, Wang XN. Experimental and theoretical study on the hot forming limit of 22MnB5 steel. *Int. J. Adv. Manuf. Technol.* **2014**, *71*, 297–306. doi:10.1007/s00170-013-5468-x.

71. Mandal G, Dey I, Mukherjee S, Ghosh SK. Phase transformation and mechanical properties of ultrahigh strength steels under continuous cooling conditions. *J. Mater. Res. Technol.* **2022**, *19*, 628–642. doi:10.1016/j.jmrt.2022.05.033.

72. Quan G, Zhan Z, Zhang L, Wu D, Luo G, Xia Y. A study on the multi-phase transformation kinetics of ultra-high-strength steel and application in thermal-mechanical-phase coupling simulation of hot stamping process. *Mater. Sci. Eng. A* **2016**, *673*, 24–38. doi:10.1016/j.msea.2016.07.010.

73. He K, Zhao X. 3D Thermal Finite Element Analysis of the SLM 316L Parts with Microstructural Correlations. *Complexity* **2018**, *2018*, 6910187. doi:10.1155/2018/6910187.

74. Tang B, Wang Q, Wei Z, Meng X, Yuan Z. FE Simulation Models for Hot Stamping an Automobile Component with Tailor-Welded High-Strength Steels. *J. Mater. Eng. Perform.* **2016**, *25*, 1709–1721. doi:10.1007/s11665-016-2011-x.

75. Ghafouri M, Ahn J, Mourujärvi J, Björk T, Larkiola J. Finite element simulation of welding distortions in ultra-high strength steel S960 MC including comprehensive thermal and solid-state phase transformation models. *Eng. Struct.* **2020**, *219*, 110804. doi:10.1016/j.engstruct.2020.110804.

76. Hou Y, Min J, El-Aty AA, Han HN, Lee M-G. A new anisotropic-asymmetric yield criterion covering wider stress states in sheet metal forming. *Int. J. Plast.* **2023**, *166*, 103653. doi:10.1016/j.ijplas.2023.103653.

77. Wang J, Bai Z, Gao Y, Shi Z, Guo Z, Li X. Study on Contact Characteristics of Cold Rolled Deformation Zone of Ultra-High-Strength Steel. *Metals* **2025**, *15*, 311. doi:10.3390/met15030311.

78. Trondl A, Sun D-Z. Modelling of Strain-Rate Dependence of Deformation and Damage Behavior of HSS- and UHSS at Different Loading States. 2015. Available online: https://lsdyna.ansys.com/wp-content/uploads/attachments/03-Trondl-FraunhoferIWM-P.pdf (accessed on 9 July 2025).

79. Priest J, Ghadbeigi H, Ayvar-Soberanis S, Liljerehn A, Way M. A modified Johnson-Cook constitutive model for improved thermal softening prediction of machining simulations in C45 steel. *Procedia CIRP* **2022**, *108*, 106–111. doi:10.1016/j.procir.2022.03.022.

80. Donadon MV, Bressan JD. Application of Barlat's Yld 2000-2d Yield Criterion to Predict the Anisotropic Response of Stainless Steel. In *Forming the Future*; Daehn G, Cao J, Kinsey B, Tekkaya E, Vivek A, Yoshida Y, Eds.; Springer International Publishing: Cham, Switzerland, 2021; pp. 749–761. doi:10.1007/978-3-030-75381-8_62.

81. Li D-H, Shang D-G, Li Z-G, Wang J-J, Hui J, Liu X-D, et al. Unified viscoplastic constitutive model under axial-torsional thermo-mechanical cyclic loading. *Int. J. Mech. Sci.* **2019**, *150*, 90–102. doi:10.1016/j.ijmecsci.2018.09.046.

82. Castillo JI, Celentano DJ, Cruchaga MA, García-Herrera CM. Characterization of strain rate effects in sheet laser forming. *Comptes Rendus Mécanique* **2018**, *346*, 794–805. doi:10.1016/j.crme.2018.05.001.

83. Song J, Jang I, Gwak S, Noh W, Lee J, Bae G, et al. Effect of Pulsed Currents on the Springback Reduction of Ultra-High Strength Steels. *Procedia Eng.* **2017**, *207*, 359–364. doi:10.1016/j.proeng.2017.10.788.

84. Bidabadi BS, Naeini HM, Tafti RA, Tajik Y. Optimization of required torque and energy consumption in the roll forming process. *Int. J. Interact. Des. Manuf.* **2019**, *13*, 1029–1048. doi:10.1007/s12008-019-00564-9.

85. Bammer F. Optimized Heat Distributions for Laser-Assisted Forming. *J. Eng.* **2024**, *2024*, 9470839. doi:10.1155/2024/9470839.

86. Farshidianfar MH, Khajepouhor A, Gerlich A. Real-time monitoring and prediction of martensite formation and hardening depth during laser heat treatment. *Surf. Coat. Technol.* **2017**, *315*, 326–334. doi:10.1016/j.surfcoat.2017.02.055.

87. Zhang X, Zhou L, Feng G, Xi K, Algadi H, Dong M. Laser technologies in manufacturing functional materials and applications of machine learning-assisted design and fabrication. *Adv. Compos. Hybrid. Mater.* **2024**, *8*, 76. doi:10.1007/s42114-024-01154-4.

88. Wei Z, Cao J, Cheng J, Wang X, Zhu H, Zhu X, et al. Precise local deformation control for UHSS thin-walled component in roll forming. *J. Manuf. Process.* **2024**, *112*, 302–312. doi:10.1016/j.jmapro.2024.01.017.

89. Jiang H, Yang Z, Guo Z, Hou J, Lei Z, Bai R, et al. Interpretation of mechanical properties gradient in laser-welded joints: Experiments and grain morphology-dependent crystal plasticity modeling. *J. Mater. Res. Technol.* **2024**, *33*, 5934–5950. doi:10.1016/j.jmrt.2024.10.226.

90. Cao Y, Zhao L, Peng Y, Song L, Zhong M, Ma C, et al. Microstructure and Mechanical Properties of Simulated Heat Affected Zone of Laser Welded Medium-Mn Steel. *ISIJ Int.* **2020**, *60*, 2266–2275. doi:10.2355/isijinternational.ISIJINT-2019-716.

91. Xue J, Peng P, Guo W, Xia M, Tan C, Wan Z, et al. HAZ Characterization and Mechanical Properties of QP980-DP980 Laser Welded Joints. *Chin. J. Mech. Eng.* **2021**, *34*, 80. doi:10.1186/s10033-021-00596-x.

92. Dong W, Bao L, Li W, Shin K, Han C. Effects of Laser Forming on the Mechanical Properties and Microstructure of DP980 Steel. *Materials* **2022**, *15*, 7581. doi:10.3390/ma15217581.

93. Singh R, Alberts MJ, Melkote SN. Characterization and prediction of the heat-affected zone in a laser-assisted mechanical micromachining process. *Int. J. Mach. Tools Manuf.* **2008**, *48*, 994–1004. doi:10.1016/j.ijmachtools.2008.01.004.

94. Chowdhury MN, Kim J, Hong S, Jung J, Han H, So S. Tailoring of Mechanical Properties of Indirect Hot Stamping Steel Tubes by Laser Assisted Local Rapid Heating. *J. Iron. Steel Res. Int.* **2016**, *23*, 949–954. doi:10.1016/S1006-706X(16)30143-1.

95. Han J, Lee Y-K. The effects of the heating rate on the reverse transformation mechanism and the phase stability of reverted austenite in medium Mn steels. *Acta Mater.* **2014**, *67*, 354–361. doi:10.1016/j.actamat.2013.12.038.

96. Arulvel S, Jain A, Kandasamy J, Singhal M. Laser processing techniques for surface property enhancement: Focus on material advancement. *Surf. Interfaces* **2023**, *42*, 103293. doi:10.1016/j.surfin.2023.103293.

97. Aboulkhair NT, Maskery I, Tuck C, Ashcroft I, Everitt NM. Improving the fatigue behaviour of a selectively laser melted aluminium alloy: Influence of heat treatment and surface quality. *Mater. Des.* **2016**, *104*, 174–182. doi:10.1016/j.matdes.2016.05.041.

98. Lee S, Ahmadi Z, Pegues JW, Mahjouri-Samani M, Shamsaei N. Laser polishing for improving fatigue performance of additive manufactured Ti-6Al-4V parts. *Opt. Laser Technol.* **2021**, *134*, 106639. doi:10.1016/j.optlastec.2020.106639.

99. Lu YJ, Zhang ZL, Liu YJ, Yu C, Zhang X, Liu XC. Improving mechanical properties and corrosion behavior of biomedical Ti-3Zr-2Sn-3Mo-25Nb alloy through laser surface remelting. *Surf. Coat. Technol.* **2024**, *490*, 131135. doi:10.1016/j.surfcoat.2024.131135.

100. Liang H, Liu J, Sun L, Hou J, Cao Z. Optimization of the Forming Quality of a Laser-Cladded AlCrFeNiW0.2 High-Entropy Alloy Coating. *Coatings* **2023**, *13*, 1744. doi:10.3390/coatings13101744.

101. Karamimoghadam M, Rezayat M, Moradi M, Mateo A, Casalino G. Laser Surface Transformation Hardening for Automotive Metals: Recent Progress. *Metals* **2024**, *14*, 339. doi:10.3390/met14030339.

102. Rashid RAR, Nazari KA, Barr C, Palanisamy S, Orchowski N, Matthews N, et al. Effect of laser reheat post-treatment on the microstructural characteristics of laser-cladded ultra-high strength steel. *Surf. Coat. Technol.* **2019**, *372*, 93–102. doi:10.1016/j.surfcoat.2019.05.021.

103. Wang Z, Dirrenberger J, Lapouge P, Dubent S. Laser treatment of 430 ferritic stainless steel for enhanced mechanical properties. *Mater. Sci. Eng. A* **2022**, *831*, 142205. doi:10.1016/j.msea.2021.142205.

104. Stewens T, Liu Y, Wang L, Min J. An analytical model for the tool center point placement in Robotic Roller Forming. *Comput. Methods Mater. Sci.* **2024**, *24*, 39–48. doi:10.7494/cmms.2024.2.0838.

105. Seyedkashi SMH, Gollo MH, Biao J, Moon YH. Laser bendability of SUS430/C11000/SUS430 laminated composite and its constituent layers. *Met. Mater. Int.* **2016**, *22*, 527–534. doi:10.1007/s12540-016-5711-8.

106. Safari M, Mostaan H, Farzin M. Laser bending of tailor machined blanks: Effect of start point of scan path and irradiation direction relation to step of the blank. *Alex. Eng. J.* **2016**, *55*, 1587–1594. doi:10.1016/j.aej.2016.01.010.

107. Kotobi M, Honarpisheh M. Through-depth residual stress measurement of laser bent steel–titanium bimetal sheets. *J. Strain Anal. Eng. Des.* **2018**, *53*, 130–140. doi:10.1177/0309324717753212.

108. Safari M, Ebrahimi M. Numerical Investigation of Laser Bending of Perforated Sheets. *Int. J. Adv. Des. Manuf. Technol.* **2016**, *9*, 53–60.

109. Dixit US, Fetene BN. A finite element modelling of laser bending of friction stir welded aluminium 5052-H32 sheets. *Int. J. Mechatron. Manuf. Syst.* **2016**, *9*, 215–236. doi:10.1504/IJMMS.2016.079589.

110. Kant R, Joshi SN. Thermo-mechanical studies on bending mechanism, bend angle and edge effect during multi-scan laser bending of magnesium M1A alloy sheets. *J. Manuf. Process.* **2016**, *23*, 135–148. doi:10.1016/j.jmapro.2016.05.017.

111. Naqvi SMR, Haidry AA, Xie D, Ahmad S, Liu Y, Chen Y, et al. Influence of laser beam process parameters on the bending ability of Ti-6Al-4V titanium alloy sheets. *Int. J. Adv. Manuf. Technol.* **2024**, *133*, 3445–3460. doi:10.1007/s00170-024-13903-2.

112. Yazici C, Domínguez-Gutiérrez FJ. Machine learning techniques for estimating high–temperature mechanical behavior of high strength steels. *Results Eng.* **2025**, *25*, 104242. doi:10.1016/j.rineng.2025.104242.

113. Pantalé O, Mha PT, Tongne A. Efficient implementation of non-linear flow law using neural network into the Abaqus Explicit FEM code. *Finite Elem. Anal. Des.* **2022**, *198*, 103647. doi:10.1016/j.finel.2021.103647.

114. Panthi SK, Ramakrishnan N, Ahmed M, Singh SS, Goel MD. Finite Element Analysis of sheet metal bending process to predict the springback. *Mater. Des.* **2010**, *31*, 657–662. doi:10.1016/j.matdes.2009.08.022.

115. Adzima F, Balan T, Manach PY. Springback prediction for a mechanical micro connector using CPFEM based numerical simulations. *Int. J. Mater. Form.* **2020**, *13*, 649–659. doi:10.1007/s12289-019-01503-5.

116. Adzima F, Balan T, Manach PY, Bonnet N, Tabourot L. Crystal plasticity and phenomenological approaches for the simulation of deformation behavior in thin copper alloy sheets. *Int. J. Plast.* **2017**, *94*, 171–191. doi:10.1016/j.ijplas.2016.06.003.

117. Brahme A, Alvi MH, Saylor D, Fridy J, Rollett AD. 3D reconstruction of microstructure in a commercial purity aluminum. *Scr. Mater.* **2006**, *55*, 75–80. doi:10.1016/j.scriptamat.2006.02.017.

118. Park T, Hector LG, Hu X, Abu-Farha F, Fellinger MR, Kim H, et al. Crystal plasticity modeling of 3rd generation multi-phase AHSS with martensitic transformation. *Int. J. Plast.* **2019**, *120*, 1–46. doi:10.1016/j.ijplas.2019.03.010.

119. Zaikovska L, Ekh M, Gupta M, Moverare J. Three-Dimensional Non-Homogeneous Microstructure Representation Using 2D Electron Backscatter Diffraction Data for Additive-Manufactured Hastelloy X. *Materials* **2024**, *17*, 5937. doi:10.3390/ma17235937.

120. Azhari F, Wallbrink C, Sterjovski Z, Crawford BR, Menzel A, Agius D, et al. Predicting the complete tensile properties of additively manufactured Ti-6Al-4V by integrating three-dimensional microstructure statistics with a crystal plasticity model. *Int. J. Plast.* **2022**, *148*, 103127. doi:10.1016/j.ijplas.2021.103127.

121. Gao Z, Zhu C, Wang C, Shu Y, Liu S, Miao J, et al. Advanced deep learning framework for multi-scale prediction of mechanical properties from microstructural features in polycrystalline materials. *Comput. Methods Appl. Mech. Eng.* **2025**, *438*, 117844. doi:10.1016/j.cma.2025.117844.

122. Liu Z, Hou Y, He R, Ye Y, Niu C, Min J. Machine learning for extending capability of mechanical characterization to improve springback prediction of a quenching and partitioning steel. *J. Mater. Process. Technol.* **2022**, *308*, 117737. doi:10.1016/j.jmatprotec.2022.117737.

123. Belitzki A, Stadter C, Zaeh MF. Distortion minimization of laser beam welded components by the use of finite element simulation and Artificial Intelligence. *CIRP J. Manuf. Sci. Technol.* **2019**, *27*, 11–20. doi:10.1016/j.cirpj.2019.10.001.